Engineering alcohol tolerance in yeast

Citation: Lam, F. H., A. Ghaderi, G. R. Fink, and G. Stephanopoulos. "Engineering Alcohol Tolerance in Yeast." Science 346, no. 6205 (October 2, 2014): 71–75.

As Published: http://dx.doi.org/10.1126/science.1257859

Publisher: American Association for the Advancement of Science (AAAS)

Persistent URL: http://hdl.handle.net/1721.1/99498

Version: Author's final manuscript: final author's manuscript post peer review, without publisher's formatting or copy editing

Title: Engineering alcohol tolerance in yeast

Authors: Felix H. Lam[1,2], Adel Ghaderi[1], Gerald R. Fink[2*], Gregory Stephanopoulos[1*]

Affiliations:

[1] Department of Chemical Engineering, Massachusetts Institute of Technology, Cambridge, Massachusetts, USA
[2] Whitehead Institute for Biomedical Research, Cambridge, Massachusetts, USA
[*] Correspondence to: G.R.F. (gfink@wi.mit.edu) or G.S. (gregstep@mit.edu)

Abstract: Ethanol toxicity in yeast *Saccharomyces cerevisiae* limits titer and productivity in the industrial production of transportation bioethanol. We show that strengthening the opposing potassium and proton electrochemical membrane gradients is a mechanism that enhances general resistance to multiple alcohols. Elevation of extracellular potassium and pH physically bolster these gradients, increasing tolerance to higher alcohols and ethanol fermentation in commercial and laboratory strains (including a xylose-fermenting strain) under industrial-like conditions. Production per cell remains largely unchanged with improvements deriving from heightened population viability. Likewise, up-regulation of the potassium and proton pumps in the laboratory strain enhances performance to levels exceeding industrial strains. Although genetically complex, alcohol tolerance can thus be dominated by a single cellular process, one controlled by a major physicochemical component but amenable to biological augmentation.

Main Text:

The increased use of renewable transportation fuels such as bioethanol is an accepted strategy to combat global climate change (*1*). However, the toxicity of ethanol and other alcohols to the yeast *Saccharomyces cerevisiae* is a primary factor limiting titer and productivity

in industrial production (*2*, *3*). Ethanol tolerance is a complex phenotype: studies have shown that no single genetic modification is capable of eliciting greater resistance at high ethanol levels (*4*-*7*).

As toxicity may arise from chemical perturbation of the plasma membrane, we surmised that ionic composition of the culture medium could play a role in exacerbating or ameliorating this destabilization (*8*-*10*). Therefore, we supplemented various salts to high cell density and high glucose cultures mimicking industrial fermentation to ascertain their consequences on ethanol production.

Monopotassium phosphate (K-P_i) added to standard yeast synthetic complete (YSC) medium induced the greatest improvement (fig. S1), an effect that we dissected into components deriving from elevated potassium (K^+) and pH. Specifically, when the pH of cultures containing elevated potassium chloride (KCl) was manually adjusted with potassium hydroxide (KOH) throughout the course of fermentation to match that of cultures containing elevated K-P_i, ethanol titers were statistically indistinguishable ($p = 0.09$ from two sample *t*-test; $p \leq 7.6\times10^{-3}$ for other pairs) from one another (fig. S2, S3). We also determined that KCl elicited a statistically higher improvement than sodium chloride (NaCl), and that supplementation with NaCl and sodium hydroxide, or with monosodium phosphate, demonstrated a distinguishable boost over NaCl alone ($p \leq 2\times10^{-4}$ from pair-wise *t*-tests). Thus, the greatest improvements in ethanol production derive specifically from the increase in K^+ concentration and reduction in acidity of the fermentation medium.

Over the course of a 3-day culture, supplementation with KCl and KOH enhanced ethanol titer and volumetric productivity (grams of ethanol per volume per hour), two key benchmarks of fermentative performance (Fig. 1A). Additionally, compared with equimolar KCl

or matched pH alone, the combination of K^+ supplementation and acidity reduction enabled the complete utilization of glucose and decreases in the synthesis of acetic acid and glycerol, two undesired byproducts of fermentation (fig. S4A–D). Ethanol titers of 115–120 g/L have been reported previously from S288C (*11*), the inbred laboratory strain used here that is known for its low ethanol resistance (*5*, *12*, *13*). However, these studies were typically conducted using chemically undefined ("rich") media. The 128±0.7 g/L (SD) concentrations observed here were achieved using a purely synthetic formulation, allowing us to identify, and precisely control, the environmental components that impact ethanol tolerance.

The boost in ethanol production from KCl and KOH supplementation did not arise simply from an increase in cell number, but from an increase in cell tolerance. Specifically, the 80±1.3% (SD) jump in titer (Fig. 1A) was accompanied only by an 11±4.6% (SD) average higher cell density (Fig. 1B); therefore, cell growth alone could not explain the rise in output. This discrepancy, however, was resolved when we directly assessed fractions of cells remaining alive throughout fermentation (fig. S5A) and discovered that the addition of KCl and KOH enhanced overall population viability (Fig. 1B, fig. S5B). This enhancement, furthermore, occurred despite the increase in toxicity imposed by higher accumulations of ethanol.

When we calculated specific productivities — rates of ethanol increase normalized by the live, rather than total, cell population — the values from KCl and KOH supplementation differed from the control by an average of 11±7.5% (SD) (Fig. 1A). That these differences account for a minor portion of the increase in titer suggests that elevated K^+ and pH acts primarily not by affecting per-cell output, but by boosting tolerance and the overall viable cell population. Additionally, these effects are observed fully in fermentations conducted in anaerobic bioreactors, demonstrating that these tolerance improvements do not depend on oxygen

availability and can scale to higher-volume environments (fig. S6).

Because it is the viable cell population that is actively fermenting, final titers are governed both by the number of live cells and the length of time over which cells maintain viability against rising ethanol toxicity. The time integral of the viable cell population captures these two aspects and quantifies the overall impact of tolerance on ethanol production (fig. S5B, S5C). Indeed, varying the concentration of supplemental KCl resulted in a dose-dependent increase of these time integrals; moreover, when these same additions were done at a higher pH, integrated viable population values were shifted upward correspondingly (Fig. 1C, fig. S7A). A strong linear relationship exists between the time integrals of viable cell density and final titers ($R^2 = 0.96$; $p = 1.5\times10^{-7}$), demonstrating that the ability to endure toxicity is a principal determinant of ethanol output and the primary trait strengthened by KCl and KOH supplementation (Fig. 1D, fig. S7B).

The enhancements conferred by elevated K^+ and reduced acidity transcend genetic background and are elicited universally among a random sampling of industrial yeast strains. Those used in the production of biofuel ethanol in Brazil (PE-2) and the United States (Lasaffre Ethanol Red), and of sake wine in Japan (Kyokai No. 7), are typically the result of genetic selection efforts designed to isolate superior ethanol phenotypes (*13-15*). Consequently, all demonstrate distinctly higher ethanol output than S288C (10±1% – 30±1.2% (SD)) when grown in unmodified medium (Fig. 2A). However, when subjected to KCl and KOH supplementation, all strains responded with enhancements in tolerance that enabled the complete consumption of glucose (fig. S8) and titers of 116±0.9 – 127±1.6 g/L (SD). Under these conditions, S288C performed indistinguishably from the two industrial bioethanol strains ($p \geq 0.08$ from pair-wise *t*-tests). Thus, a strain traditionally deemed ethanol sensitive is inherently capable — without

genetic modification — of superior tolerance, indicating that K^+ supplementation and acidity reduction drive a process that can supersede advantages conferred by genetic adaptation.

These adjustments to the medium, furthermore, enhance fermentation from xylose, an important hemicellulosic sugar that cannot be consumed by standard strains of *S. cerevisiae*. In an engineered strain (*16*), 22±0.9 g/L (SD) ethanol was produced from unmodified medium containing 100 g/L xylose (Fig. 2A). When fermented with the addition of KCl and KOH, we observed a 54±5.7% (SD) increase in titer, commensurate with the complete assimilation of xylose (fig. S8). Thus, K^+ supplementation and acidity reduction enhance tolerance in a manner impartial to the type of substrate.

The improvements conferred by elevated K^+ and pH generalize beyond synthetic media to chemically undefined broths, provided that such formulations do not already saturate for these effects. For example, in yeast extract-peptone (YP) medium (~pH 6 and unknown concentrations of individual nutrients (*17*)), cells ferment all sugar such that no margin is available for improvement (fig. S9B). However, the impact of specific supplements can be assessed if the YP components are made limiting. Indeed, when YP was decreased to 30% or 3% while maintaining the same glucose concentration, supplementation with K^+ improved ethanol output whereas additives shown to be fermentation-neutral (from fig. S1) did not (fig. S9A). Using YP diluted to 20%, titers of 104±0.8 g/L (SD) are produced, while the addition of K^+ enhanced output 17±2.5% (SD) (Fig. 2B). When pH was reduced from 6 to 3.7, production was concomitantly reduced 28±0.8% (SD). However, the subsequent addition of K^+ compensated for this decrease, restoring titers 47±2.5% to 109±1.8 g/L (SD). Thus, in media with undefined composition, extracellular K^+ and pH are also sufficient to quantitatively modulate ethanol performance.

To isolate the effects of KCl and KOH supplementation on tolerance from other fermentation variables (e.g., decreasing turgor pressure from glucose consumption), we subjected yeast to non-physiological step increases in ethanol concentration and quantified population fractions surviving after 80 min, a period much shorter than the length of fermentation but adequate for cell viability to be impacted. In medium containing a subsistence amount of glucose that minimizes newly produced ethanol, elevated K^+ and pH enhanced viability in shocks up to 27% (vol/vol) when compared to cells stressed in unmodified conditions (Fig. 2C). Analogous experiments performed using high glucose (mimicking the osmotic conditions of high gravity fermentation) and heightened K-P_i yielded a similar result, albeit at a lower range of ethanol concentrations (fig. S10A). These results indicate that the impact of elevated K^+ and reduced acidity is relatively immediate, does not require adaptation to ethanol accumulation over the course of days, and is capable of overcoming the combined stress of high sugar and ethanol (*2*).

The boost in tolerance conferred by heightened K^+ and pH extends to higher alcohols capable of serving as unmodified substitutes for gasoline. Although at lower concentrations when compared to ethanol (reflecting their increased toxicity), we observed that viability is similarly enhanced when cells are shocked using step increases of isopropanol and isobutanol (Fig. 2D, 2E, fig. S10B). That the improvements are not unique to ethanol suggest that these adjustments to the medium augment a more general cellular process involved in alcohol resistance or membrane integrity.

Given the dominant effects exerted by extracellular K^+ and pH, we hypothesized that K^+ and proton (H^+) regulation may be a primary mechanism mediating the tolerance phenotype. Because opposing gradients of K^+ and H^+ ions are generated across the yeast plasma membrane

by the K^+ importer *TRK1* and H^+ exporter *PMA1* (*18*, *19*), we surmised that genetic modifications of these ATP-dependent pumps, designed to perturb or strengthen these gradients, would produce corresponding effects to fermentative performance. Indeed, genetic deletions that debilitate K^+ import or H^+ export weakened ethanol output (fig. S11). Likewise, hyper-activation of *TRK1*, accomplished by deletions of *PPZ1* and *PPZ2* (*19*), generated an increase, yielding an 18±1.6% (SD) improvement in titer over the wild type when cultured in unmodified medium (Fig. 3, fig. S12A). Given the electroneutral co-dependence of the K^+ and H^+ gradients (*18*), we, furthermore, reasoned that up-regulation of *PMA1* alongside augmented *TRK1* would further enhance the ethanol phenotype; indeed, the combination increased titers by 27±2.2% (SD) over the wild type. These improvements in output mirrored enhancements in net fermentation viability (fig. S12B), affirming the coupled nature of production and tolerance. Incidentally, over-expression of *PMA1* without hyper-activation of *TRK1* did not enhance ethanol performance (Fig. 3), supporting the proposed notion that K^+ uptake creates the dominant electromotive force and H^+ efflux acts primarily as a response current (*19*).

Genetic augmentation of the K^+ and H^+ transporters increased ethanol titer of the laboratory strain to that surpassing the two bioethanol production strains (Fig. 3). These specific genetic modifications are, therefore, sufficient to create a superior phenotype previously available only through selection. That hyper-activation of *TRK1* alone is sufficient to match the titers of PE-2 and Ethanol Red, combined with the observation that these industrial strains respond to KCl and KOH supplementation, lends support to the possibility that polymorphisms enhancing the K^+ and H^+ gradients may be responsible for intrinsically higher ethanol tolerances (*20*).

Collectively, our results suggest a toxicity model where alcohols attack viability not at

threshold concentrations that solubilize lipid bilayers, but at lower concentrations that increase permeability of the plasma membrane and dissipate the cell's ionic membrane gradients. That genetically unchanged cells can be made to tolerate higher ethanol concentrations by modulating extracellular K^+ and pH indicates that many observed tolerance thresholds (e.g., the sub-100 g/L titers from unmodified medium) represent a physiological, rather than chemical, limit. Ethanol has been known to decrease intracellular pH in a dose-dependent fashion, demonstrating that its amphipathicity permeabilizes the plasma membrane to H^+ (and, potentially, other ions) (*8*, *21*). Furthermore, that the coupled K^+ and H^+ gradients comprise a dominant portion of the yeast electrical membrane potential, used to power many of the cell's exchange processes with the environment, hints that the cessation of nutrient and waste transport due to gradient dissipation may be a primary mode of cell death (*18*, *21-25*).

These ionic gradients are likely disrupted with increasing strength as ethanol accumulates during fermentation, requiring the cell to expend escalating amounts of energy to reestablish the steep separation of charges. Conditions that bolster the cell's efforts to maintain high concentrations of intracellular K^+ and low intracellular H^+ (estimated to be 200–300 mM and pH 7, respectively (*23*, *24*)) thus likely enhance tolerance by raising the threshold to which alcohols will collapse these gradients (Fig. 4). Physical reinforcements in the form of K^+ supplementation and acidity reduction generate the greatest improvements: not only do higher concentrations of extracellular K^+ facilitate import (by potentially reducing the gradient from 36- to 4-fold, using the above estimates), and lower concentrations of extracellular H^+ facilitate export, the corresponding rates of ion leakage are decreased due to reduced concentration differences across the membrane. Likewise, genetic modifications strengthening the ion pump activities responsible for establishing the K^+ and H^+ gradients increase performance without alteration of

the medium. However, that KCl and KOH supplementation confers larger improvements suggests that tolerance may contain a considerable physically driven component that ultimately constrains biological augmentation.

Figure Captions:

Fig. 1. Elevated extracellular potassium and pH enhance ethanol tolerance and production under high glucose and high cell density conditions. (A) Ethanol titers (squares) and per-cell rates of production (triangles) from fermentations in unmodified synthetic complete medium (YSC; dashed) or YSC supplemented with 40 mM KCl and 10 mM KOH (solid). Specific productivities are calculated from the mean viable population (thick lines from **B**) during each 24 h period. **(B)** Cell densities (dry cell weight/DCW; thin squares) and the underlying viable populations (thick triangles) from the fermentations in **A**. Data are mean ± SD from 3 biological replicates. **(C)** Net fermentation viability, expressed as time integrals of the viable cell population, as a function of potassium added to YSC in the form of KCl (pH 3.6), or 5 mM KOH + KCl (pH 5.8). **(D)** Time integral values from **C** regressed against their final ethanol titers.

Fig. 2. Elevated potassium and pH are sufficient to enhance tolerance independently of strain genetics, sugar substrate, and alcohol species. (A) Ethanol titers from glucose fermentation (top) of one laboratory (S288C) and three industrial (PE-2, Ethanol Red, Kyokai 7) yeast strains, or from xylose fermentation (bottom) of an engineered xylose strain, in unmodified YSC or YSC supplemented with 40 mM KCl and 10 mM KOH. **(B)** Titers from S288C cultured in 20% yeast extract-peptone medium (YP) or that supplemented with potassium, at pH 6 and 3.7. **(C)** Population fractions of S288C after transfer from overnight growth in unmodified YSC

(dashed), or that supplemented with 48 mM KCl and 2 mM KOH (solid), into media containing the indicated concentrations of ethanol. **(D, E)** Same as **C**, but with step increases of isopropanol or isobutanol, respectively. All data are mean ± SD from 3 biological replicates.

Fig. 3. Genetic augmentation of the plasma membrane potassium (*TRK1*) and proton (*PMA1*) pumps increase ethanol production to levels exceeding industrial strains. Ethanol titers from a wild type laboratory strain (S288C) transformed with empty over-expression plasmid, S288C transformed with a plasmid over-expressing *PMA1*, S288C containing hyper-activated *TRK1* (via deletions of *PPZ1* and *PPZ2*) and transformed with empty over-expression plasmid, the *TRK1* hyper-activated strain transformed with a plasmid over-expressing *PMA1*, and bioethanol production strains from Brazil (PE-2) and the US (Ethanol Red), all cultured in unmodified YSC lacking uracil. Data are mean ± SD from 3 biological replicates.

Fig. 4. Potential biophysical mechanism depicting how elevated potassium and pH counteract rising alcohol toxicity. In the absence of stress (top row), the opposing potassium (K^+) and proton (H^+) pumps maximally maintain steep gradients of K^+ and H^+ across the plasma membrane. Rising alcohol levels perturb these gradients by permeabilizing the membrane and increasing ion leakage (middle left). Elevated potassium and pH, however, bolster the gradients by slowing rates of ion leakage (due to reduced concentration differences) and allowing transporters to pump against a less precipitous differential (middle right). Therefore, the threshold alcohol concentration that collapses these gradients is raised, allowing cells to maintain viability at higher toxicity levels (bottom row). Red corresponds to K^+, blue to H^+, size of triangles to concentration gradient steepness, and thickness of arrows to magnitude of ion flux.

References and Notes:

1. A. L. Demain, *J Ind Microbiol Biotechnol*. **36**, 319–332 (2009).

2. F. W. Bai, L. J. Chen, Z. Zhang, W. A. Anderson, M. Moo-Young, *J Biotechnol*. **110**, 287–293 (2004).

3. G. Stephanopoulos, *Science*. **315**, 801–804 (2007).

4. F. van Voorst, J. Houghton-Larsen, L. Jønson, M. C. Kielland-Brandt, A. Brandt, *Yeast*. **23**, 351–359 (2006).

5. S. Swinnen *et al.*, *Genome Res*. **22**, 975–984 (2012).

6. D. Stanley, A. Bandara, S. Fraser, P. J. Chambers, G. A. Stanley, *J Appl Microbiol*. **109**, 13–24 (2010).

7. H. Alper, J. Moxley, E. Nevoigt, G. R. Fink, G. Stephanopoulos, *Science*. **314**, 1565–1568 (2006).

8. A. Madeira *et al.*, *FEMS Yeast Res*. **10**, 252–258 (2010).

9. A. N. Dickey, R. Faller, *Biophys J*. **92**, 2366–2376 (2007).

10. J. Chanda, S. Bandyopadhyay, *Langmuir*. **22**, 3775–3781 (2006).

11. T. M. Pais *et al.*, *PLoS Genet.* **9**, e1003548 (2013).

12. J. A. Lewis, I. M. Elkon, M. A. McGee, A. J. Higbee, A. P. Gasch, *Genetics*. **186**, 1197–1205 (2010).

13. J. L. Argueso *et al.*, *Genome Res*. **19**, 2258–2270 (2009).

14. T. Akao *et al.*, *DNA Res.* **18**, 423–434 (2011).

15. T. Katou, M. Namise, H. Kitagaki, T. Akao, H. Shimoi, *J. Biosci. Bioeng.* **107**, 383–393 (2009).

16. H. Zhou, J.-S. Cheng, B. L. Wang, G. R. Fink, G. Stephanopoulos, *Metab Eng*. **14**, 611–622 (2012).

17. F. Sherman, *Meth Enzymol*. **350**, 3–41 (2002).

18. L. Yenush, S. Merchan, J. Holmes, R. Serrano, *Mol Cell Biol*. **25**, 8683–8692 (2005).

19. L. Yenush, J. M. Mulet, J. Ariño, R. Serrano, *EMBO J*. **21**, 920–929 (2002).

20. C. Reisser *et al.*, *G3 (Bethesda)* (2013), doi:10.1534/g3.113.005884.

21. C. P. Cartwright *et al.*, *Microbiology*. **132**, 369–377 (1986).

22. R. Madrid, M. J. Gómez, J. Ramos, A. Rodríguez-Navarro, *J Biol Chem*. **273**, 14838–14844 (1998).

23. R. Orij, S. Brul, G. J. Smits, *Biochim Biophys Acta*. **1810**, 933–944 (2011).

24. M. S. Cyert, C. C. Philpott, *Genetics*. **193**, 677–713 (2013).

25. J. Horák, *Biochim Biophys Acta*. **1331**, 41–79 (1997).

Acknowledgments: We are grateful to present and former members of the Fink and Stephanopoulos labs for intellectual and technical guidance. Additionally, we thank V. Vyas and D. Pincus for critical commentary on the manuscript, and Phibro for the gift of Lesaffre Ethanol Red. Support was provided by the MIT Energy Initiative and Dept. of Energy grant DE-SC0008744 to G.S., and National Institutes of Health grant R01-GM035010 to G.R.F. No competing financial interests impinged on this study. F.H.L., G.R.F., and G.S. are listed as co-inventors on a patent application filed by MIT and the Whitehead Institute. F.H.L., G.R.F., and G.S. designed all experiments and collaborated on the manuscript; A.G. conducted all bioreactor studies; F.H.L. performed all other experiments, strain construction, and analysis of data. Supporting data are available in the supplementary materials.

Fig. 1A

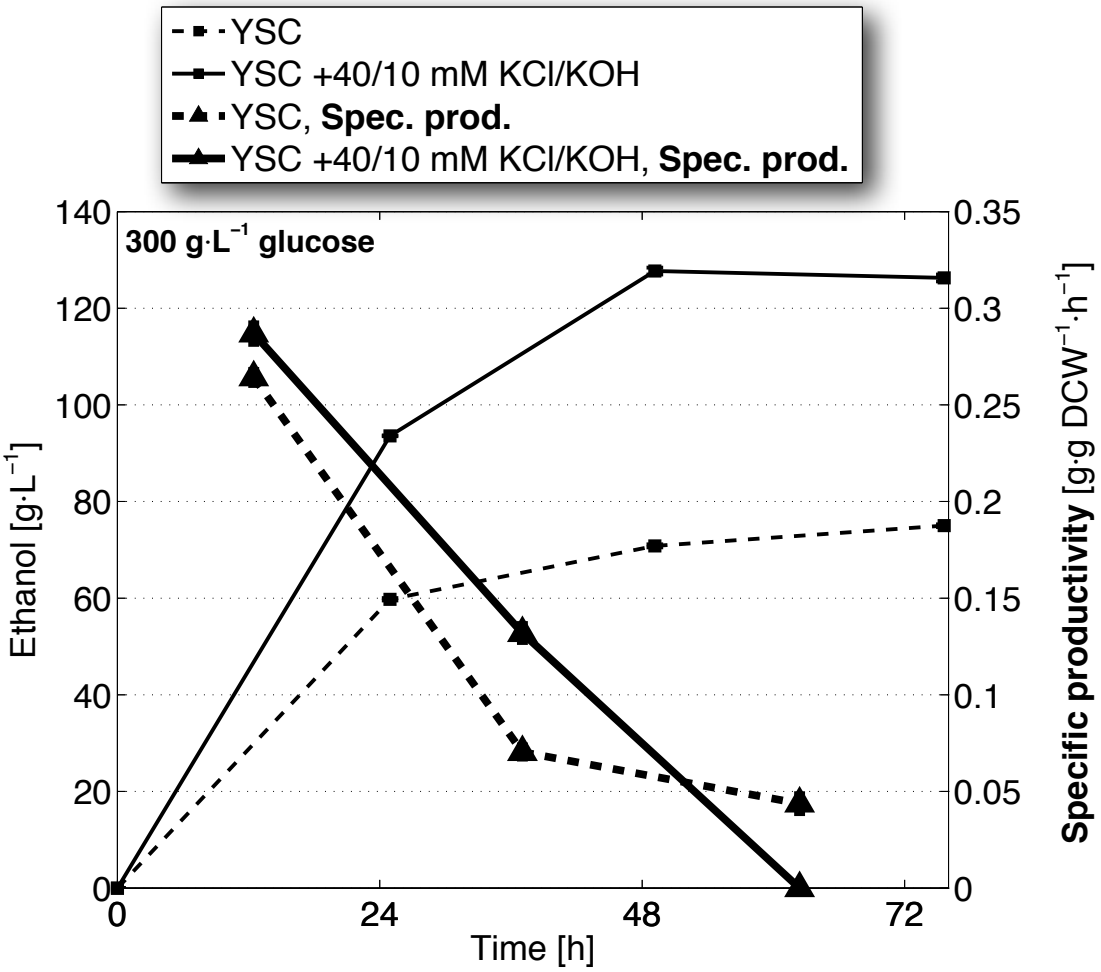
YSC
YSC +40/10 mM KCl/KOH
YSC, Spec. prod.
YSC +40/10 mM KCl/KOH, Spec. prod.
300 g·L⁻¹ glucose
Ethanol [g·L⁻¹]
Specific productivity [g·g DCW⁻¹·h⁻¹]
Time [h]
0
20
40
60
80
100
120
140
0.05
0.1
0.15
0.2
0.25
0.3
0.35
24
48
72

Fig. 1B

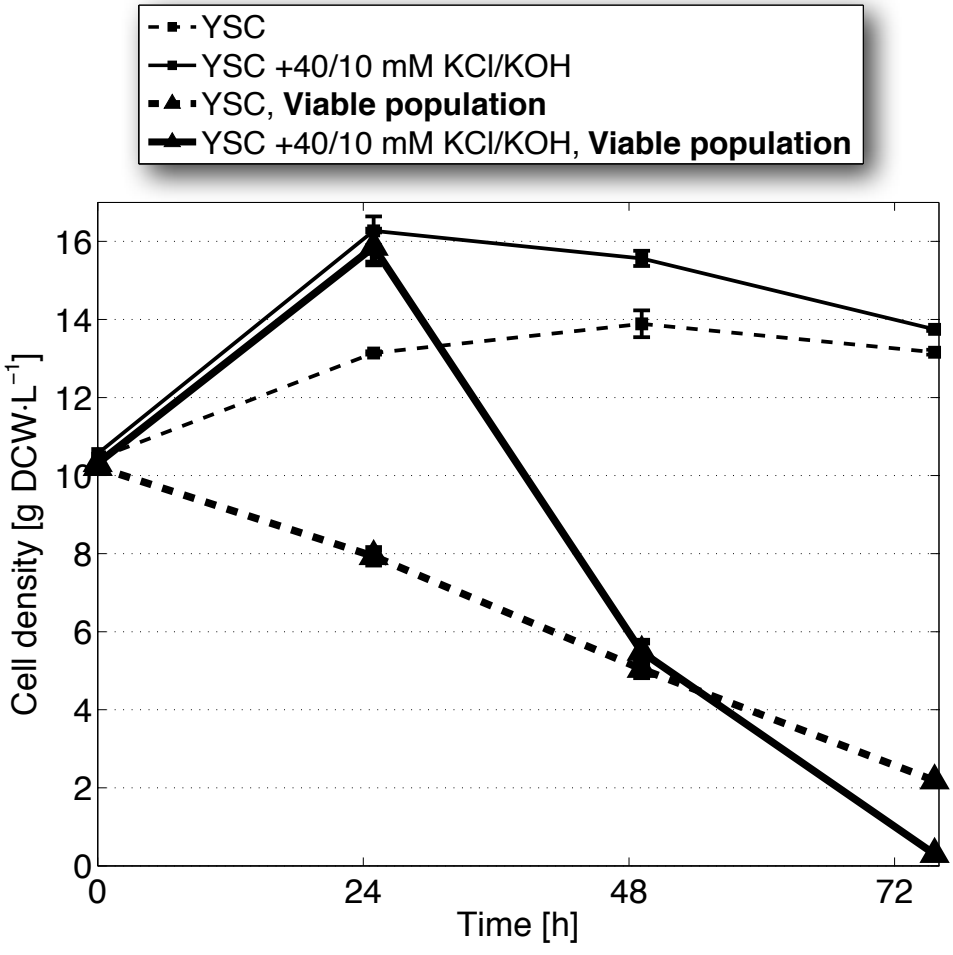
YSC
YSC +40/10 mM KCl/KOH
YSC, Viable population
YSC +40/10 mM KCl/KOH, Viable population
Cell density [g DCW·L⁻¹]
Time [h]
0
2
4
6
8
10
12
14
16
24
48
72

Fig. 1C

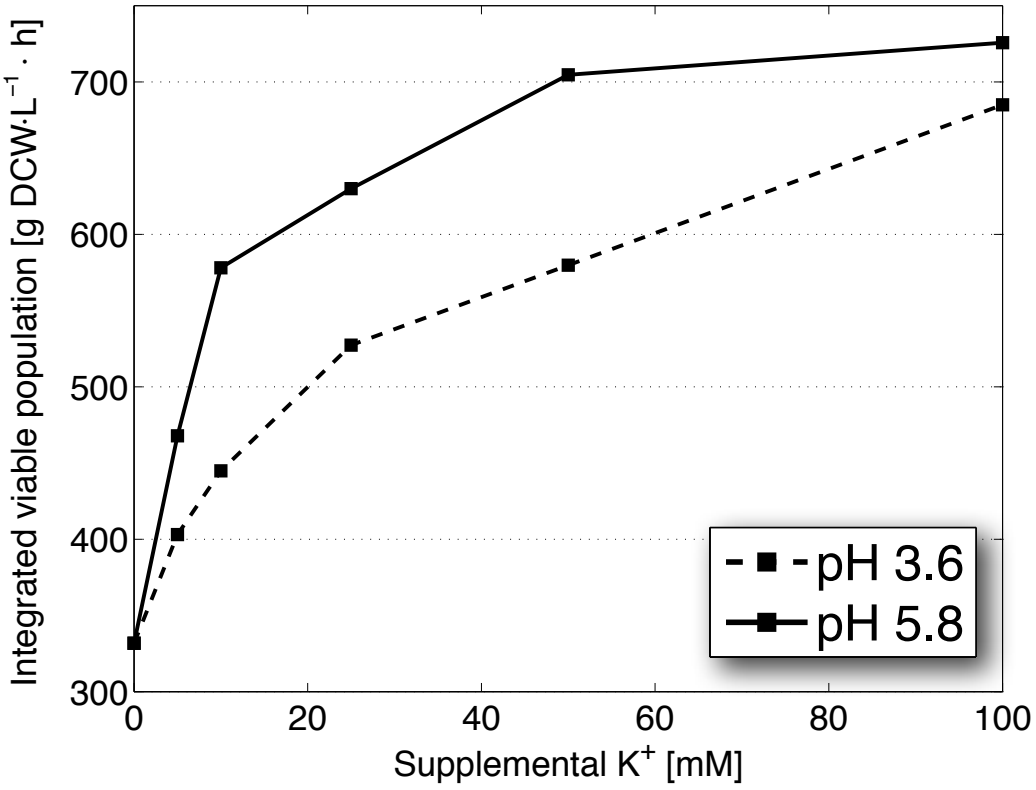
Integrated viable population [g DCW·L^{-1} · h]
700
600
500
400
300
0
20
40
60
80
100
Supplemental K^{+} [mM]
pH 3.6
pH 5.8

Fig. 1D

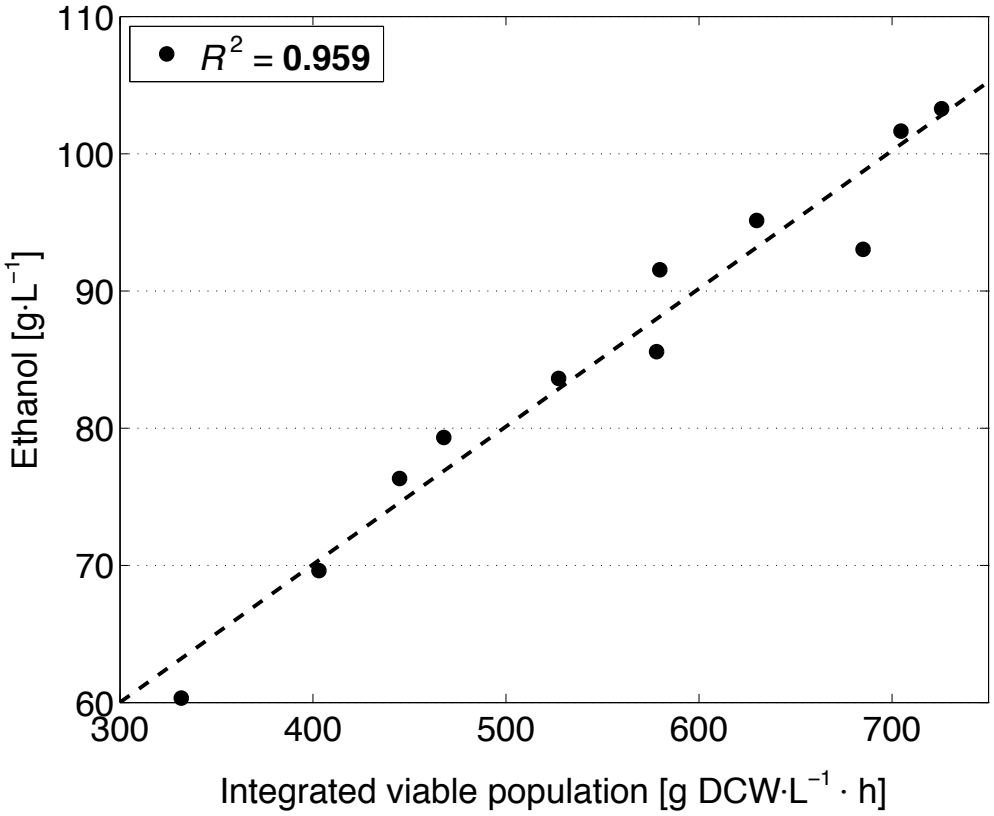
R^2 = **0.959**
Ethanol [g·L^{-1}]
110
100
90
80
70
60
300
400
500
600
700
Integrated viable population [g DCW·L^{-1} · h]

Fig. 2A

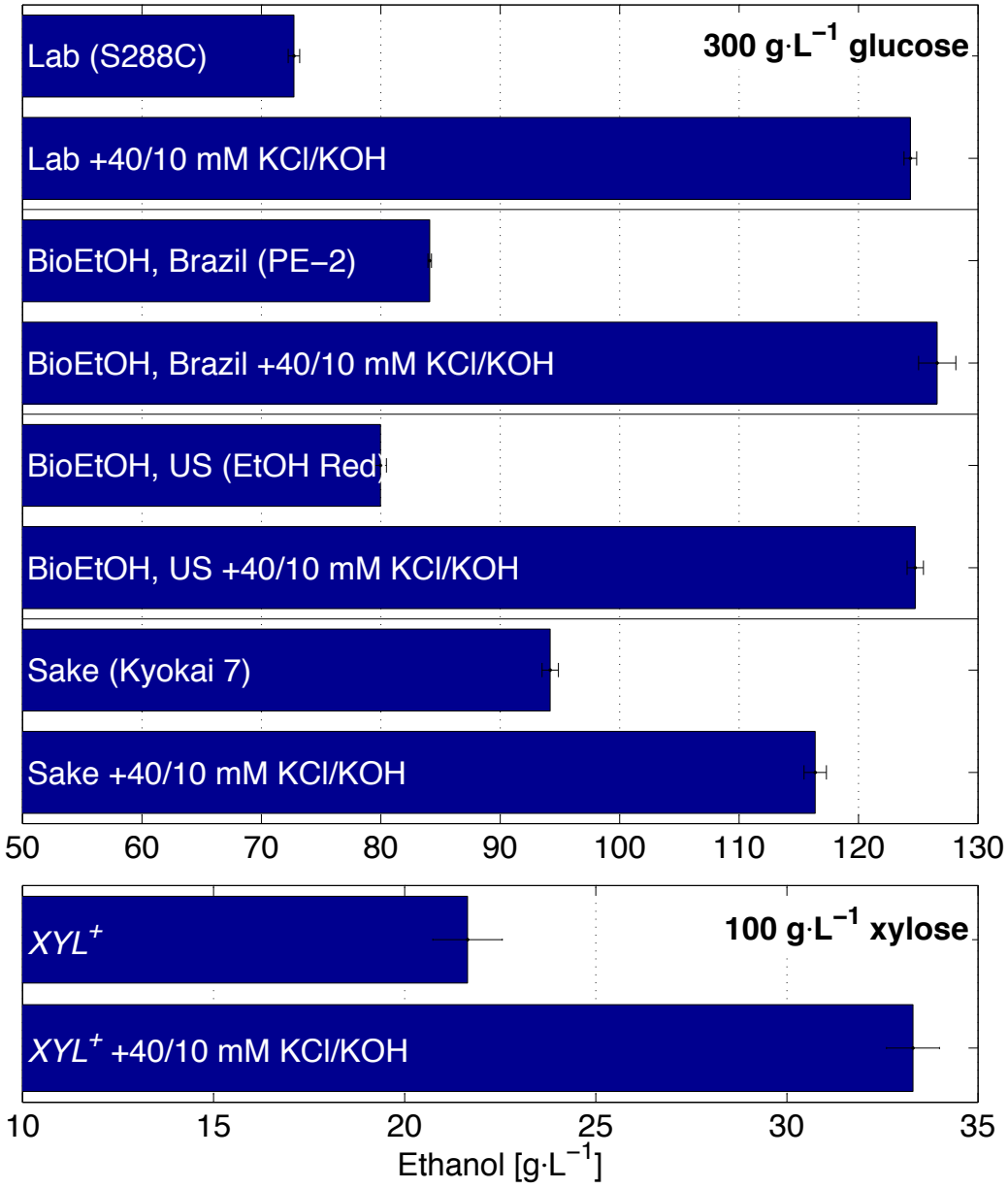
Lab (S288C)
300 g·L−1 glucose
Lab +40/10 mM KCl/KOH
BioEtOH, Brazil (PE−2)
BioEtOH, Brazil +40/10 mM KCl/KOH
BioEtOH, US (EtOH Red)
BioEtOH, US +40/10 mM KCl/KOH
Sake (Kyokai 7)
Sake +40/10 mM KCl/KOH
50 60 70 80 90 100 110 120 130
XYL+
100 g·L−1 xylose
XYL+ +40/10 mM KCl/KOH
10 15 20 25 30 35
Ethanol [g·L−1]

Fig. 2B

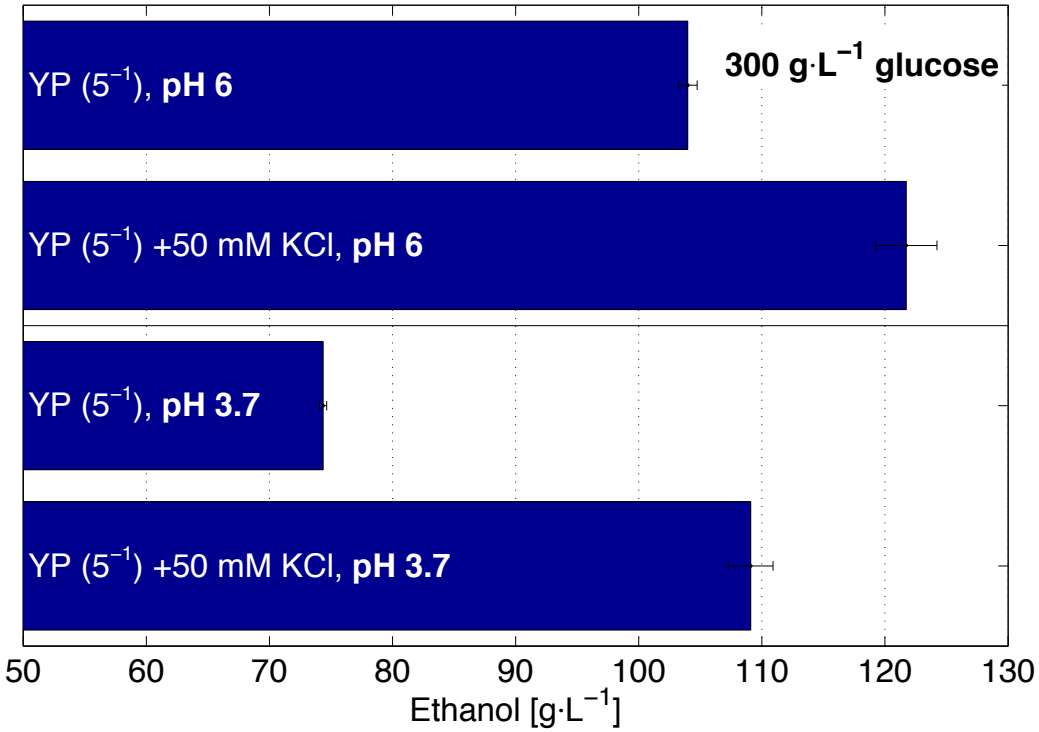
YP (5−1), pH 6
300 g·L−1 glucose
YP (5−1) +50 mM KCl, pH 6
YP (5−1), pH 3.7
YP (5−1) +50 mM KCl, pH 3.7
50 60 70 80 90 100 110 120 130
Ethanol [g·L−1]

Fig. 2C

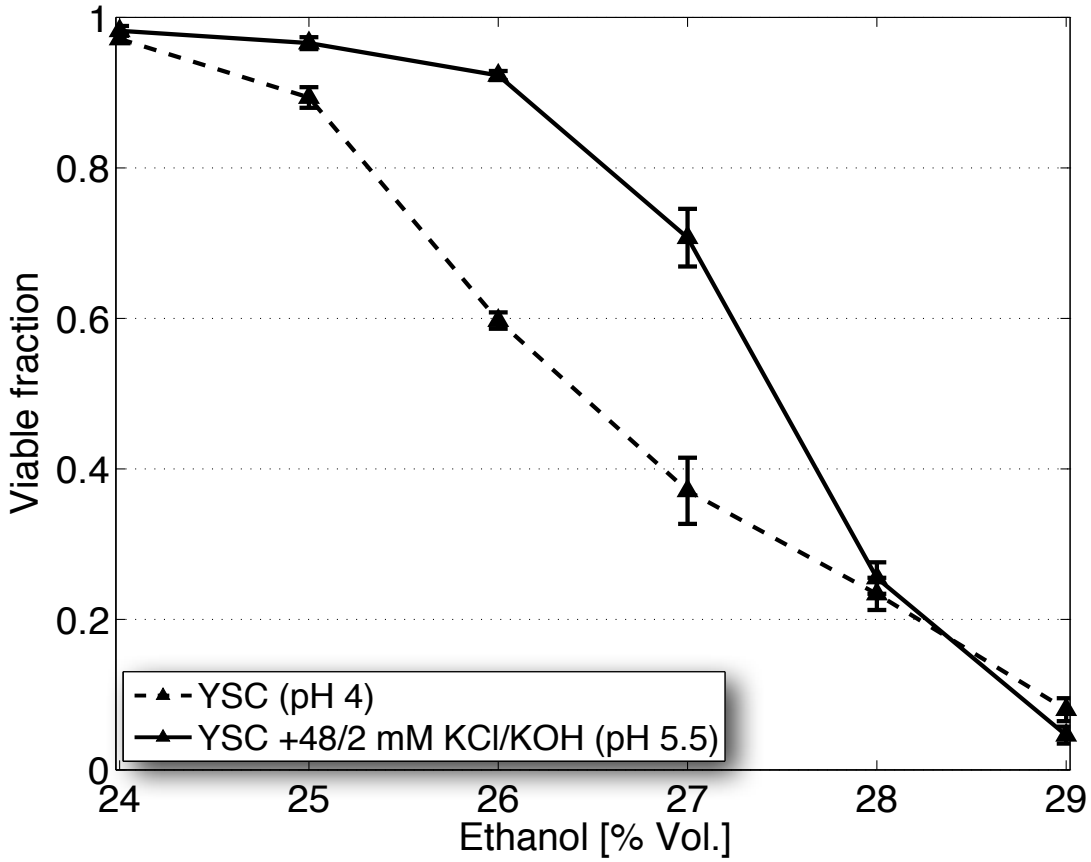
Viable fraction
Ethanol [% Vol.]
YSC (pH 4)
YSC +48/2 mM KCl/KOH (pH 5.5)
0
0.2
0.4
0.6
0.8
1
24
25
26
27
28
29

Fig. 2D

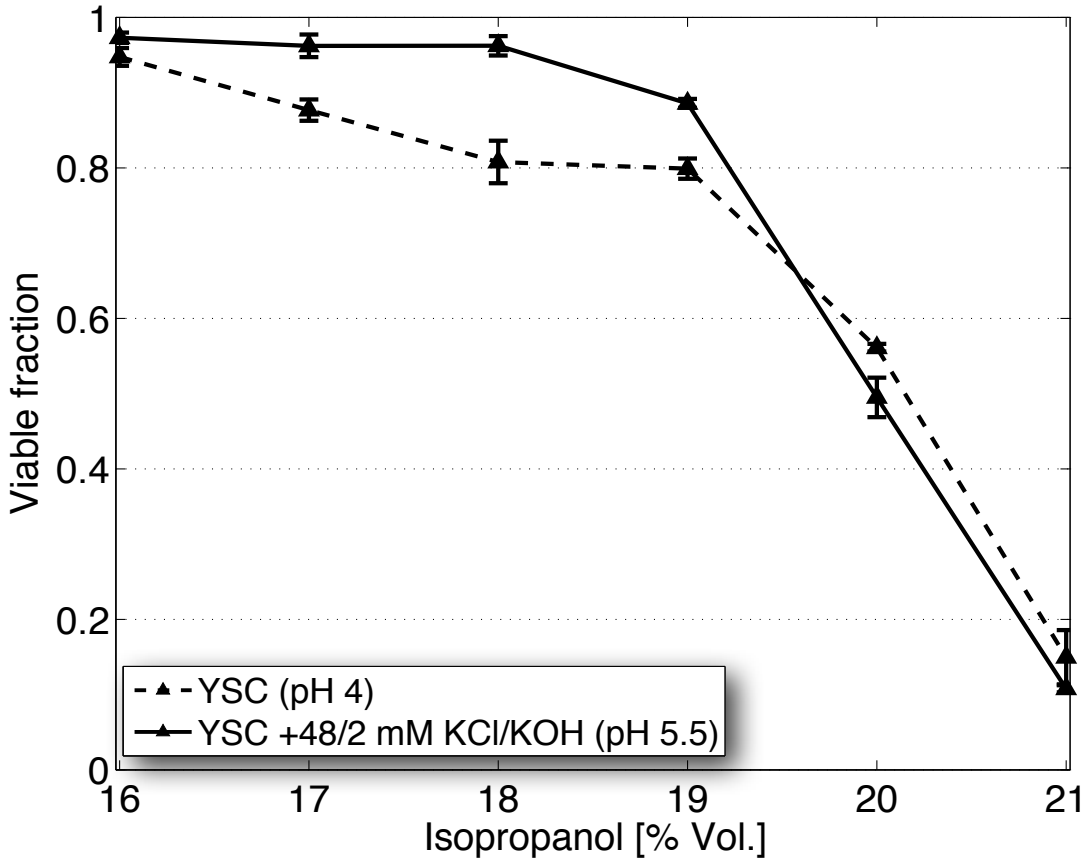
Viable fraction
Isopropanol [% Vol.]
YSC (pH 4)
YSC +48/2 mM KCl/KOH (pH 5.5)
0
0.2
0.4
0.6
0.8
1
16
17
18
19
20
21

Fig. 2E

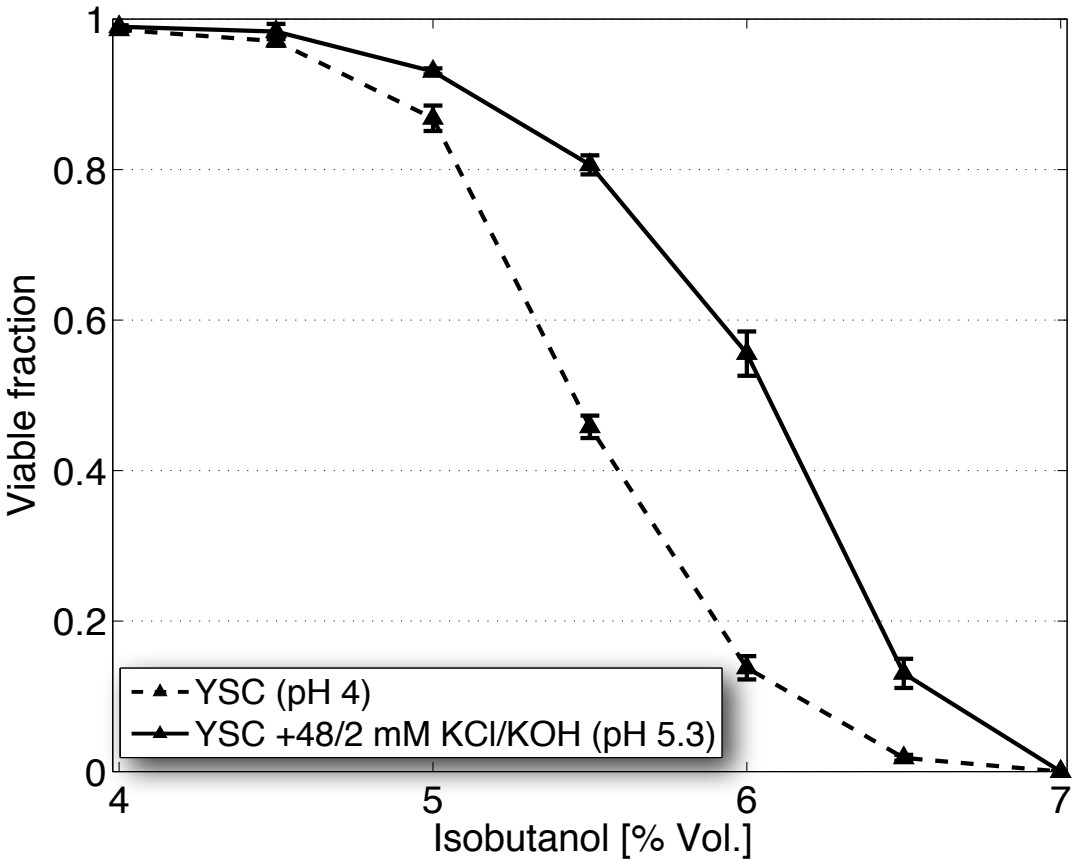
Viable fraction
1
0.8
0.6
0.4
0.2
0
4
5
6
7
Isobutanol [% Vol.]
YSC (pH 4)
YSC +48/2 mM KCl/KOH (pH 5.3)

Fig. 3

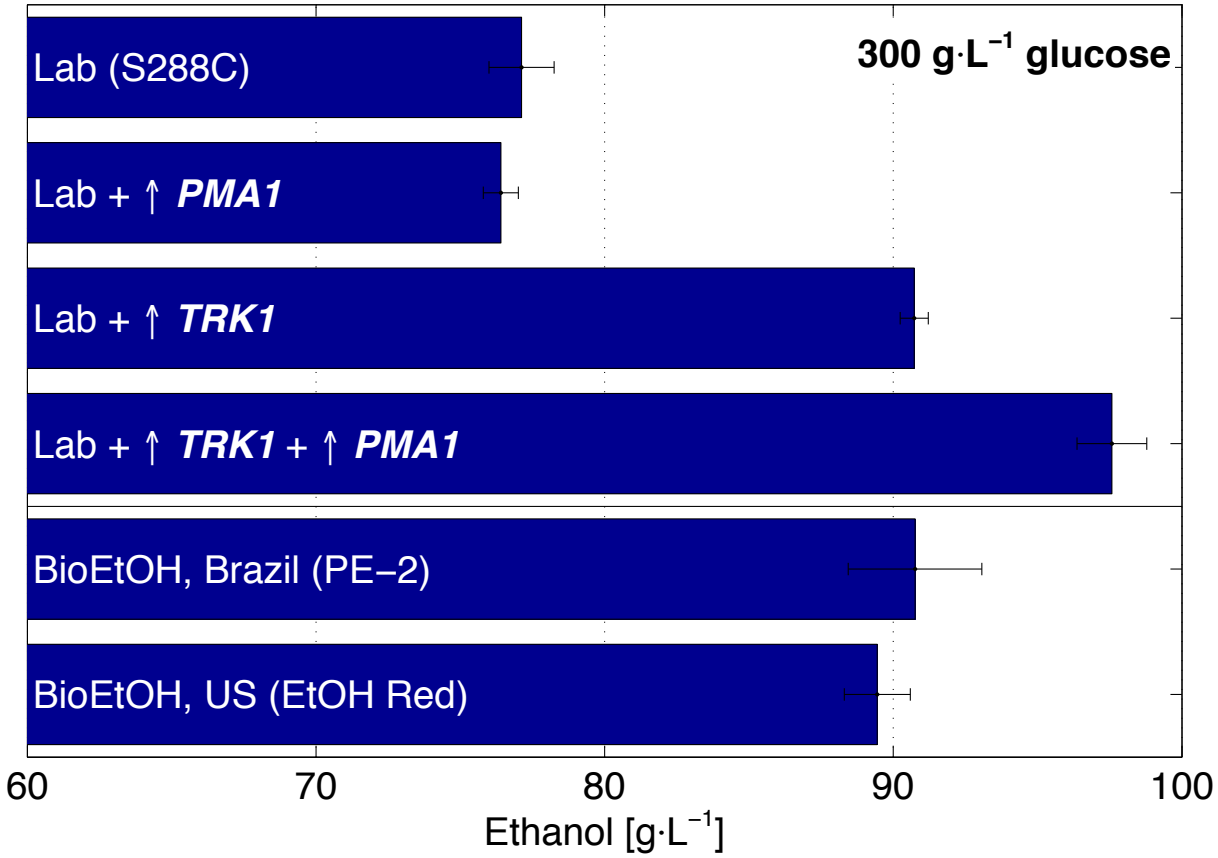
300 g·L⁻¹ glucose
Lab (S288C)
Lab + ↑ PMA1
Lab + ↑ TRK1
Lab + ↑ TRK1 + ↑ PMA1
BioEtOH, Brazil (PE–2)
BioEtOH, US (EtOH Red)
60
70
80
90
100
Ethanol [g·L⁻¹]

Fig. 4

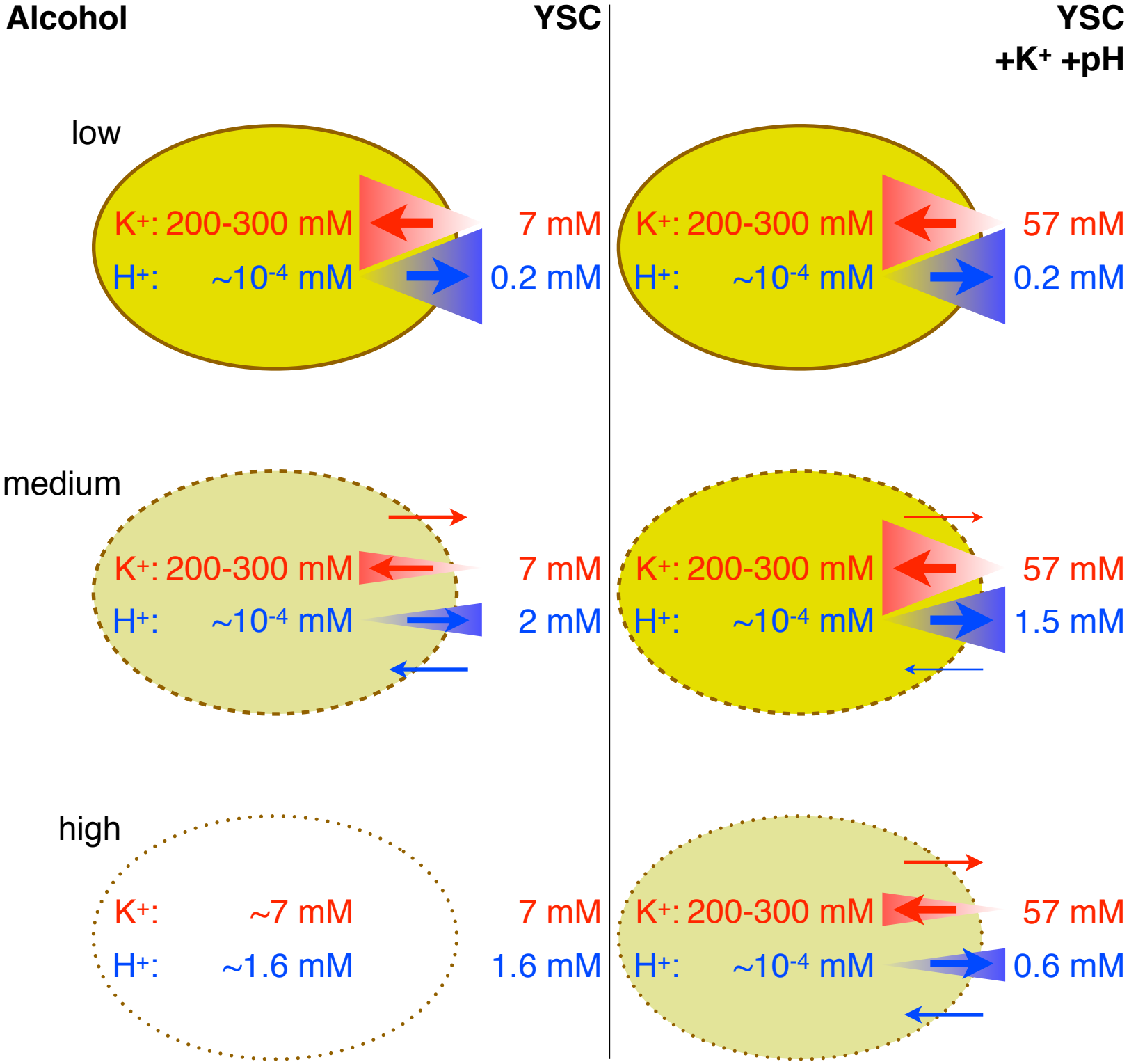
Alcohol
YSC
YSC
+K+ +pH
low
K+: 200-300 mM
H+: ~10-4 mM
7 mM
0.2 mM
K+: 200-300 mM
H+: ~10-4 mM
57 mM
0.2 mM
medium
K+: 200-300 mM
H+: ~10-4 mM
7 mM
2 mM
K+: 200-300 mM
H+: ~10-4 mM
57 mM
1.5 mM
high
K+: ~7 mM
H+: ~1.6 mM
7 mM
1.6 mM
K+: 200-300 mM
H+: ~10-4 mM
57 mM
0.6 mM

SUPPLEMENTARY MATERIALS

for

"Engineering alcohol tolerance in yeast"

Felix H. Lam, Adel Ghaderi, Gerald R. Fink*, Gregory Stephanopoulos*

* Correspondence to: G.R.F. (gfink@wi.mit.edu) or G.S. (gregstep@mit.edu)

Contents

Materials and Methods

Determination of dry cell weight. Dry cell weight (DCW) was determined by vacuum filtration using 0.2 µm cellulose nitrate membrane filters (Whatman #10401312, http://www.gelifesciences.com/Whatman). For each measurement, the filter was pre-weighed with hundredth mg precision using a Mettler Toledo microbalance (#AX105, http://www.mt.com), inserted into a vacuum flask, and wet with deionized water. A 1 mL sample was deposited and washed twice with an equal volume of deionized water. Final weight was determined after drying for 16 h in a 70°C oven. DCW was measured at five points during the course of fermentation for which optical density (OD_{600}) was also measured. For each time point, 1 mL of fresh medium was also measured (control) and any change in weight was subtracted from weight changes of other filter samples at that time point. All measurements were performed in duplicate including controls. DCW was found to correspond to OD_{600} as 0.396 ± 0.025 g $DCW \cdot L^{-1} \cdot OD_{600}^{-1}$.

Yeast strains. To generate homozygous double deletions of *PPZ1* and *PPZ2*, the *MAT*a *ppz1*Δ and *MAT*α *ppz2*Δ haploids were sourced from the Saccharomyces Genome Deletion Project collection (Life Technologies, http://clones.invitrogen.com/cloneinfo.php?clone=yeast), and mated to produce the diploid strain *ppz1*Δ::kanMX4 / *PPZ1 ppz2*Δ::kanMX4 / *PPZ2*. This heterozygote was sporulated, and ascospores dissected onto yeast extract-peptone-dextrose (YPD) plates containing 200 µg/mL G418 (Sigma-Aldrich #A1720, http://www.sigmaaldrich.com). Haploids that germinated from tetrads exhibiting a 2:2 segregation pattern unambiguously harbored the kanMX4 deletion cassette at both the *PPZ1* and

PPZ2 loci (*17*). The genotypes of these G418-resistant haploids were further verified by PCR using promoter- and kanMX4-specific primers, and subsequently assayed for mating type via the halo test for pheromone production (using tester strains F1441 and L4564 sensitive to α- and a-factor, respectively) (*26*). Haploids of the opposite mating type were then crossed to produce the homozygous double deletion strain LAMy177.

To create plasmid-carrying yeast strains, transformation of DNA was performed following the lithium acetate-based protocol of Gietz (*27*). Typically, 500 ng of URA3-encoding plasmid was introduced into 2–3 OD_{600} units (0.8–1.2 g DCW) of yeast cells grown to mid-logarithmic phase. Transformants were recovered through uracil prototrophy and further verified for the presence of the exogenous DNA by PCR using primers specific to the plasmid.

See Table S1 for a complete list of yeast strains used in this study.

Plasmid construction. All plasmids used in this study were based on the yeast p426TEF high copy over-expression vector of Mumberg (*28*). To clone *PMA1*, a 5' primer encoding a SpeI restriction site and a 3' primer encoding an XhoI site were used to amplify the *PMA1* coding sequence from BY4743 genomic DNA. Amplification reactions were performed using the Phusion high-fidelity polymerase (New England Biolabs #M0530L, http://www.neb.com) in 50 µl volumes containing HF buffer, and thermocycled using the routine 3 step program for 35 iterations in accordance with the manufacturer's instructions. Approximately 3 µg of both the p426TEF vector and ethanol-precipitated *PMA1* amplicon were double digested with SpeI (New England Biolabs #R0133L) and XhoI (New England Biolabs #R0146L) for 3 h. Linearized p426TEF was immediately dephosphorylated with alkaline phosphatase (New England Biolabs #M0290L) for 1 h at 37°C and purified via gel extraction using the QIAquick Gel Extraction Kit

(QIAGEN #28706, http://www.qiagen.com). The digested *PMA1* insert was column purified using the QIAquick PCR Purification Kit (QIAGEN #28106).

Ligation of *PMA1* to p426TEF was performed using a minimum 5 insert:1 vector molar ratio in a 20 µl reaction with T4 DNA ligase (New England Biolabs #M0202L) according to the manufacturer's instructions; however, twice the recommended amount of enzyme was used. Reaction mixtures were transformed into chemically competent NEB 5αF'I^q *E. coli* (New England Biolabs #C2992H), and ampicillin-resistant colonies screened for successful ligations by PCR using backbone- and gene-specific primers. Candidate plasmids were purified from *E. coli* cultures using the QIAprep Spin Miniprep Kit (QIAGEN #27106), and Sanger sequenced to evaluate fidelity of the ligation products.

See Table S2 for a complete list of plasmids used in this study.

Media and fermentation conditions. Unless noted otherwise, yeast strains were cultured in synthetic complete medium (YSC) made from Yeast Nitrogen Base (BD-Difco #233520, http://www.bd.com) and amino acids and remaining additives from Sigma-Aldrich (*17*). For conditions requiring plasmid maintenance, YSC lacking uracil (YSC –URA) was used. For fermentations using yeast extract-peptone (YP) medium, undiluted formulations contained the standard 10 g/L yeast extract (BD-Difco #212750) and 20 g/L peptone (BD-Difco #211830) (*17*), while dilutions contained these two components decreased in proportion (e.g., 2 g/L yeast extract + 4 g/L peptone in the 20% dilution).

All yeast cultures were incubated at 30°C with agitation. Cultures ≥ 25 mL were grown in Erlenmeyer flasks on a platform shaker set at 200 RPM, and cultures ≤ 12 mL in glass tubes on a roller drum at the maximum rotational setting.

To build yeast biomass and adapt cells osmotically for high cell density and high sugar fermentations, starter cultures consisting of unmodified medium (i.e., YSC, YSC –URA, or YP dilution) and 0.33× the target fermentation sugar concentration (e.g., 100 g/L glucose) were grown until saturation, pelleted by centrifugation, and the entire cell mass used to inoculate a "pre-fermentation" culture of the same medium and 0.5–0.66× the target sugar concentration (e.g., 150 g/L glucose). Pre-fermentation cultures were grown until saturation, washed once in the same volume of fresh medium to remove residual ethanol, re-suspended in fresh medium, and cell densities (of an appropriate dilution) determined by absorbance at 600 nm. Equalized quantities of cells were then harvested by centrifugation, re-suspended in fermentation medium to yield a starting cell density of approximately OD_{600} = 25 (9.9 g DCW/L), and divided into triplicate 12 mL samples. Fermentation media contained the target high concentration of sugar (300 g/L glucose or 100 g/L xylose), as well as any supplements under evaluation (e.g., 40 mM KCl).

For the adjustment of pH during fermentation (Fig. 1A–B, 2A, S2, S4, S5, S8, S11), a total of 10 mM potassium hydroxide (KOH) was added in the following amounts and times: 2 mM at 3, 6, 12 h; 1.5 mM at 24, 36 h; and 1 mM at 48 h. Equal amounts of water were added to unmodified YSC fermentations to control for changes in volume. In fermentations dissecting the component effects of potassium (K^+) and pH (fig. S4, S5), equal amounts of KCl were added in lieu of KOH at the same time points. To monitor pH, acidity of the fermentation medium was measured directly using a Thermo Scientific Orion 2-STAR pH meter (#1111001, http://www.thermoscientific.com) with AquaPro electrode (#9156APWP). Cross contamination was minimized by immersing the pH probe in HCl, pH 1 for several minutes and rinsing thoroughly with ddH_2O (double distilled via Millipore Milli-Q system) between samples.

Fermentations assessing the quantitative effect of K^+ concentration and pH on ethanol tolerance and production (Fig. 1C–D, S7) were modified from the above as follows. In lieu of pH adjustments made during the course of fermentation, cells were inoculated directly into media prepared with supplemental 5–100 mM KCl ("pH 3.6"), or that prepared with supplemental 5 mM KOH and 5–95 mM KCl ("pH 5.8"). Furthermore, because these data were intended specifically for regression analysis, samples were collected in singlicate. First, we reasoned that the statistical power provided by n=10 for regression was sufficient such that the necessity for triplicates was minimized. Second, because fermentations performed in YSC exhibit low variability (e.g., Fig. 1A, 2A), we felt that the prospect of handling 3× the samples would, in fact, introduce more error than managing 10 samples. Finally, the 10 data points shown were all collected in a single experiment; thus, day-to-day variability was nonexistent. Overall, when viewed in the context of regression analysis, we decided that spanning a larger range of K^+/pH conditions was more important than variability information.

Fermentations comparing the laboratory strains with augmented K^+ and/or H^+ gradients to industrial bioethanol strains (Fig. 3) were also modified as follows. To maximize expression of the up-regulated K^+ and H^+ pumps, all pre-fermentation cultures were maintained in logarithmic phase ($OD_{600} \leq 3$ or 1.2 g DCW/L) for ≥ 24 h instead of grown until saturation. Equalized quantities of each strain were harvested, re-suspended in unmodified synthetic fermentation medium to yield a target cell density of $OD_{600} = 20$ (7.9 g DCW/L), and aliquoted into triplicate samples.

All fermentations were conducted micro-aerobically: 12 mL cultures had approximately two volumes of headspace and were capped snugly with snap-on plastic tops but not sealed with Parafilm. Samples were taken every ~24 h for analysis over the course of 1–3 d. Typically, 20

µL of cells were removed and diluted 50^{-1} for measurement of cell density at OD_{600}, another 20 µL for quantification of cell viability by methylene blue staining (see below), and 0.5 mL of supernatant saved for determination of ethanol, glucose, acetic acid, and glycerol concentrations by HPLC (see below). Figures displaying final ethanol titers (e.g., Fig. 2, 3) show ethanol concentrations in the medium at the conclusion of fermentation (72 h).

See Table S3 for a summary of yeast strains and fermentation conditions used in each of this study's figures.

Ethanol, glucose, acetic acid, and glycerol determination. Concentrations of ethanol, glucose, acetic acid, and glycerol were quantified chromatographically on 0.5 mL of undiluted sample using an Agilent 1200 Series HPLC (http://www.chem.agilent.com) equipped with an Agilent 1260 Infinity Refractive Index Detector (#G1362A RID) and Aminex HPX-87H Ion Exclusion Column (Bio-Rad #125-0140, http://www.bio-rad.com). Using a 5 mM sulfuric acid mobile phase at 35°C and flow rate of 0.6 mL/min, ethanol eluted at a retention time of ~20.5 min, glucose at ~8.8 min, acetic acid at ~15.2 min, and glycerol at ~13.1 min. To determine concentrations, peak areas auto-determined by the Agilent Chemstation for LC software were interpolated off a 6 point standard curve consisting of 0–20% ethanol, 0–10% glucose, 0–3% acetic acid, and 0–0.5% glycerol (all vol/vol) prepared in YSC medium.

Viability measurements. To assess population viability, methylene blue (Sigma-Aldrich #M9140; 10 mg/mL stock prepared in ddH_2O) was added directly to aliquots of undiluted high cell density cultures to a final concentration of 1 mg/mL, and visualized immediately at 400× magnification on a Nikon Eclipse TS100 by bright field microscopy (*29*). Images were recorded

using a SPOT Insight 2 MP Firewire color camera with SPOT 5.0 software, and analyzed offline.

For each image, the number of unstained (live) cells was quantified along with the total number of cells to determine the viable population fraction. A minimum of 250 cells was counted per replicate, and error statistics calculated from the viable fractions of at least 3 replicates. Cell density measurements were multiplied by their respective viable fractions (and their standard deviations propagated) to arrive at the underlying viable population in cell density units (e.g., Fig. 1B).

All image processing and numerical analysis, including time integration of the viable cell populations, were done in MATLAB (The MathWorks, http://www.mathworks.com).

Alcohol shock tolerance assay. To isolate and quantify the ability of elevated K^+ and pH to increase resistance to sudden changes in external alcohol concentration, cells were pre-adapted to high cell density and low glucose conditions before treatment with alcohol. To build cell biomass, starter cultures of FY4/5 were grown until saturation in YSC containing 50 g/L glucose. One half of the culture was centrifuged and re-suspended in YSC containing 20 g/L glucose, the other centrifuged and re-suspended in identical medium supplemented with 48 mM KCl and 2 mM KOH, and both cultured for at least 16 h to deplete glucose (verified by HPLC; data not shown). Approximately 30 OD_{600} units (11.9 g DCW) of cells were then harvested in 2 mL screw cap tubes (in triplicate per alcohol concentration), washed with YSC containing 5 g/L glucose or that supplemented with 48 mM KCl and 2 mM KOH, respectively, and finally re-suspended in media of the same composition containing 24–29% ethanol, 16–21% isopropanol, or 4–7% isobutanol. Samples were incubated at room temperature on a rotator and assayed for viability by methylene blue staining after 80 min. The subsistence amount of 5 g/L glucose had

been chosen to minimize the contribution of any newly-produced ethanol (made during the course of the assay) to the imposed alcohol load.

However, to more closely mimic the osmotic conditions of high gravity fermentation, alcohol shock tolerance assays were also conducted in high glucose. These experiments were modified from the above as follows. Starter cultures of FY4/5 were grown until saturation in YSC containing 100 g/L glucose, divided in half, pelleted by centrifugation, re-suspended in either YSC or YSC +50 mM K-P_i containing 300 g/L glucose, and cultured for at least 12 h. Approximately 30 OD_{600} units (11.9 g DCW) of biomass were then harvested in triplicate 2 mL screw cap tubes, washed twice in respective fresh medium to remove accumulated ethanol, and re-suspended in medium of the same composition containing 10–20% ethanol (fig. S10A) or 4–14% isopropanol (fig. S10B). Samples were incubated at room temperature on a rotator, and viability assayed after 2:15 h for ethanol or 4 h for isopropanol. It is worth noting that, given the high glucose and high cell density conditions, any new ethanol that may be produced during the incubation period prior to viability assessment did not appear to negatively impact the enhancement conferred by elevated K^+ and pH.

Specific productivity. To calculate ethanol productivities per viable cell, rates of increase in ethanol titer over a specific period were normalized by the average viable cell density during the same period:

$$\frac{\mathrm{EtOH}_t - \mathrm{EtOH}_{t-1}}{\left(\frac{\mathrm{DCW}_{viable,t} + \mathrm{DCW}_{viable,t-1}}{2}\right)(t - t_{-1})} \ [\mathrm{g \cdot g\ DCW^{-1} \cdot h^{-1}}]$$

Error bars on specific productivity values were calculated from the standard deviations of the ethanol and viable cell density measurements using standard rules of uncertainty propagation.

Phosphate measurements. Concentrations of inorganic phosphate in fermentation media (fig. S2A) were assayed colorimetrically using the Malachite Green Phosphate Assay kit (ScienCell #8118, http://www.sciencellonline.com) according to the manufacturer's instructions on samples diluted 3000^{-1}.

Anaerobic bioreactor fermentations. Bioreactor fermentations were performed using a New Brunswick Scientific BioFlo 110 Bioreactor (http://newbrunswick.eppendorf.com/) using a 1 L vessel. Dissolved oxygen (DO) and pH probes were calibrated according to the manufacturer's instructions. Cells were suspended in 500 mL (working volume) YSC medium containing 300 g/L glucose and 40 mM KCl. Anaerobic conditions are achieved within 25 min of inoculation. Continuous reading from the DO probe confirmed that anaerobicity was maintained throughout the remainder of fermentation. Manual injections totaling 10 mM KOH were added to the reactor at 3, 6, 12, 24, and 36 h using 167 μL of 6 N KOH.

Statistical analysis. Computation of standard deviations, propagation of error, uni- and bivariate analyses of variance (ANOVA), two sample *t*-testing, and calculation of p values were all performed on biological triplicate measurements using functions from MATLAB or the Statistics Toolbox for MATLAB (The MathWorks). Linear regression modeling of viable population integrals and final ethanol titers (Fig. 1D) was also performed using the Statistics Toolbox for MATLAB. Error estimation on derived values (e.g., means, percent changes) were calculated from the standard deviations of primary measurements using standard rules of uncertainty propagation.

Discussion

Genetic debilitation of K^+ and H^+ transport. We employed genetic deletions to determine if hindering K^+ import or H^+ export weakens ethanol performance. Both a complete ablation of *TRK1* and partial ablation of *PMA1* (a homozygous deletion is lethal (*30*, *31*)) decreased titers relative to the wild type when cultured in unmodified medium (fig. S11). However, as elevated K^+ and pH are capable of increasing ethanol performance in a manner dominant to strain genetics (Fig. 2A), we found that KCl and KOH supplementation rescued, and largely nullified, these genetic impairments (fig. S11).

Elevated K^+ and pH, and nutrient depletion. We determined that supplementation with KCl and KOH does not relieve a general nutritional deficiency that may be triggered by high cell density. To address this possibility, we conducted fermentations with low cell density (initial OD_{600} = 0.1 or 0.04 g DCW/L) and, additionally, repeated these conditions with the addition of 3% ethanol to impose a mild ethanol stress at the start of fermentation. In both scenarios, nutrients remained in abundance, yet we still observed improved ethanol performance with the addition of KCl alone or with the combination of KCl and KOH (fig. S13). Thus, elevated K^+ and pH likely participate in a process specific to withstanding ethanol stress and do not alleviate resource constraints that may be created by overpopulation.

References

26. G. F. Sprague, Assay of yeast mating reaction. *Meth Enzymol* **194**, 77–93 (1991).

27. R. D. Gietz, R. H. Schiestl, A. R. Willems, R. A. Woods, Studies on the transformation of intact yeast cells by the LiAc/SS-DNA/PEG procedure. *Yeast* **11**, 355–360 (1995).

28. D. Mumberg, R. Müller, M. Funk, Yeast vectors for the controlled expression of heterologous proteins in different genetic backgrounds. *Gene* **156**, 119–122 (1995).

29. K. A. Smart, K. M. Chambers, I. Lambert, C. Jenkins, C. A. Smart, Use of methylene violet staining procedures to determine yeast viability and vitality. *Journal of the American Society of Brewing Chemists* **57**, 18–23 (1999).

30. R. Serrano, M. C. Kielland-Brandt, G. R. Fink, Yeast plasma membrane ATPase is essential for growth and has homology with (Na+ + K+), K+- and Ca2+-ATPases. *Nature* **319**, 689–693 (1986).

31. C. H. Ko, R. F. Gaber, TRK1 and TRK2 encode structurally related K+ transporters in Saccharomyces cerevisiae. *Mol Cell Biol* **11**, 4266–4273 (1991).

Fig. S1

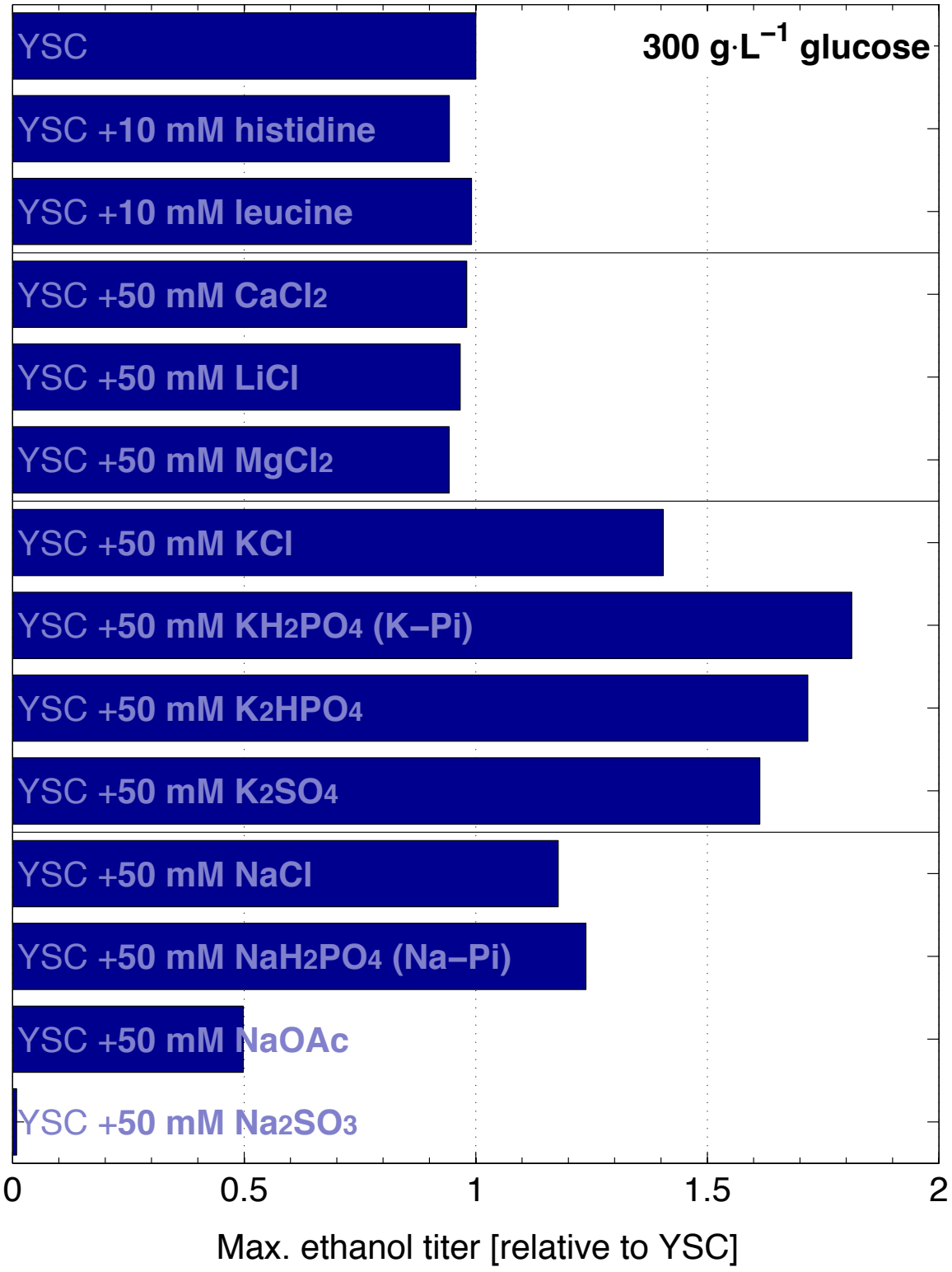

Fig. S1. Media supplementation with potassium-based salts exerts the largest improvement on ethanol output, with 50 mM monopotassium phosphate (K-P_i) eliciting the greatest increase. The S288C laboratory prototroph was cultured for 72 h in synthetic complete medium (YSC) containing 300 g/L glucose and the indicated additives, all equalized for initial pH (3.8) and cell density (OD_{600} = 25 or 9.9 g DCW/L).

Fig. S2 A)

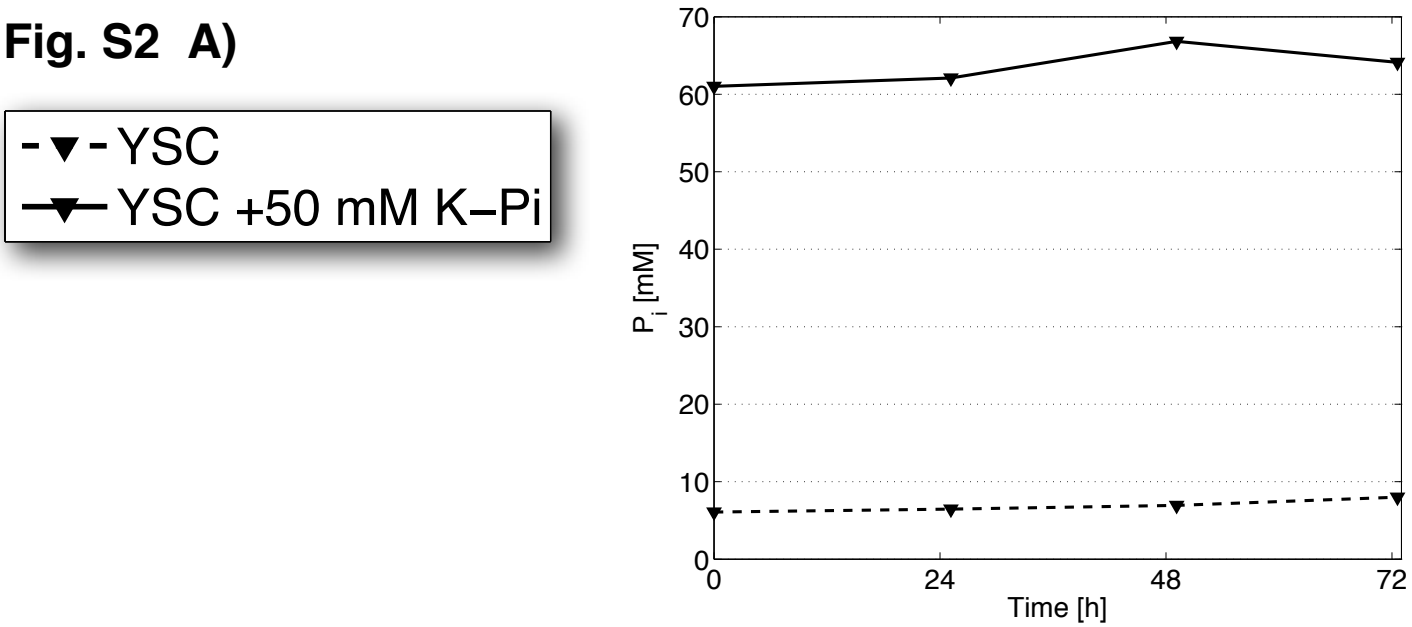

B)

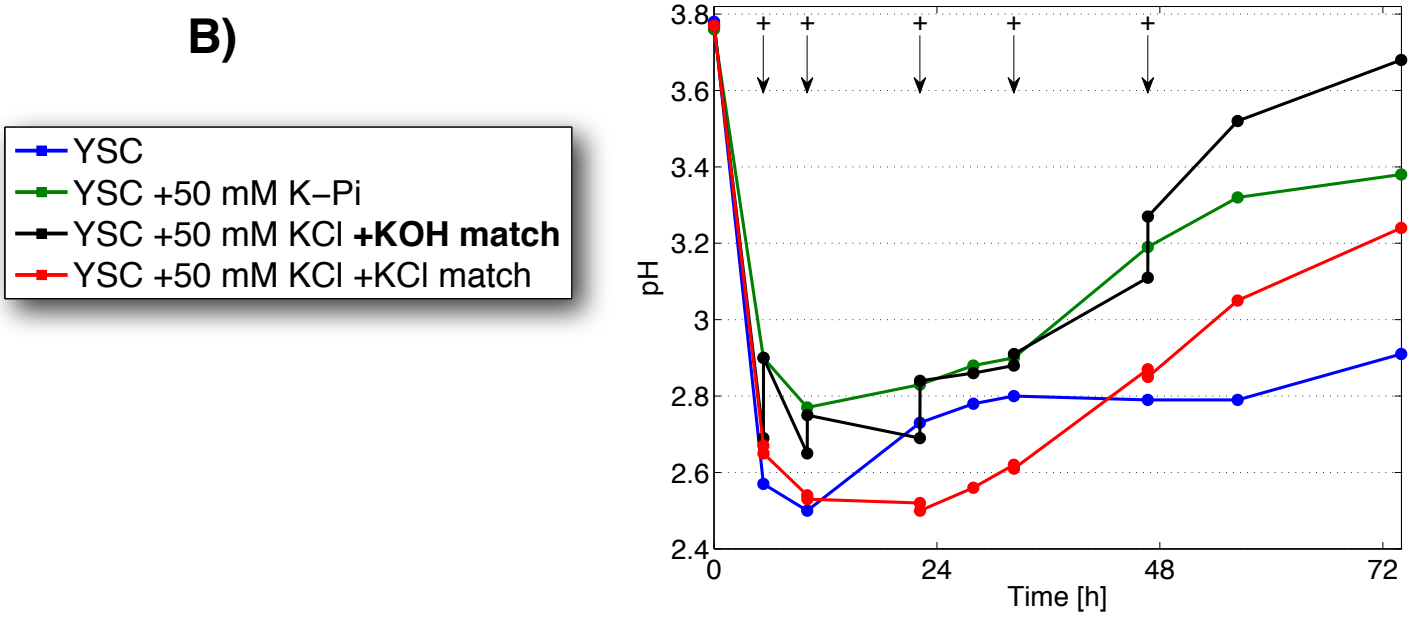

C)

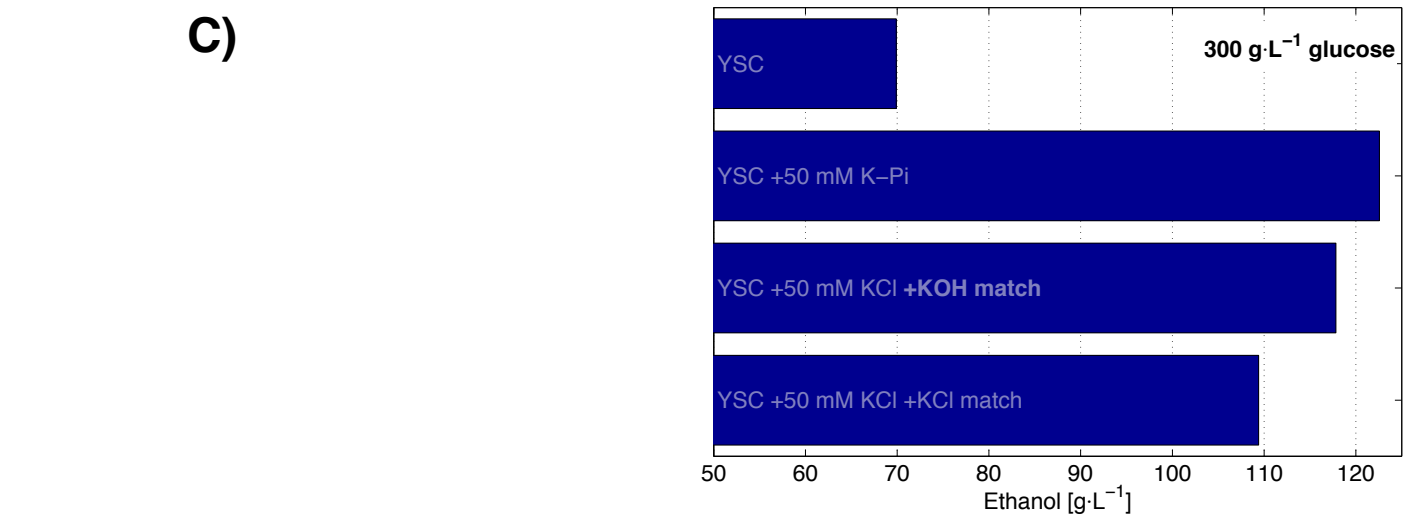

Fig. S2. Supplemental K-P_i enhances ethanol fermentation, not by alleviating phosphate depletion, but by raising pH of the medium. **(A)** Concentrations of inorganic phosphate measured throughout fermentation in unmodified YSC (dashed) or YSC supplemented with 50 mM K-P_i (solid). **(B)** Fermentation pH in unmodified YSC (blue), YSC supplemented with 50 mM K-P_i (green), with 50 mM KCl and periodic additions of KOH to match that of elevated K-P_i (black), or with 50 mM KCl and periodic additions of KCl equimolar to the added KOH (red). **(C)** Final ethanol titers of the fermentations in **B**.

Fig. S3

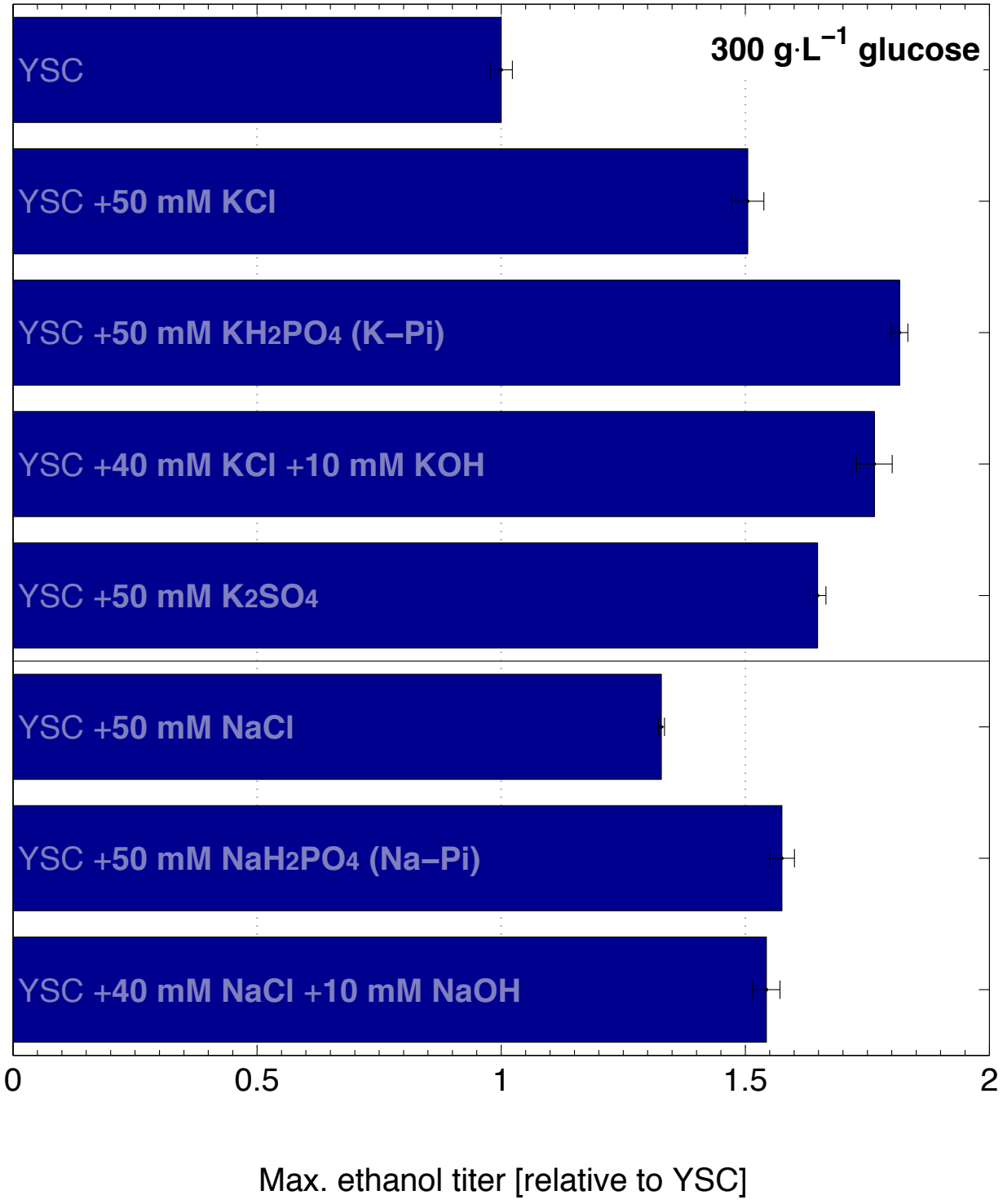

Fig. S3. Relative ethanol titers and analysis of variance (ANOVA) of biological triplicate fermentations conducted using YSC and the indicated supplements. Univariate ANOVA of fermentations supplemented with 50 mM K-P_i are inseparable from those with matched potassium and pH (40 mM KCl+10 mM KOH; $p = 0.092$), but statistically higher than those with other potassium-based salts ($p \leq 7.58\times10^{-3}$). Similarly, fermentations supplemented with 50 mM Na-P_i are indistinguishable from those with matched sodium and pH (40 mM NaCl+10 mM NaOH; $p = 0.217$), but higher than those with NaCl alone ($p \leq 1.96\times10^{-4}$). Bivariate ANOVA confirms that the increase conferred by potassium over sodium is significant ($p = 5.1\times10^{-7}$), while that of phosphate vs. raised pH is insignificant ($p = 0.031$).

Fig. S4

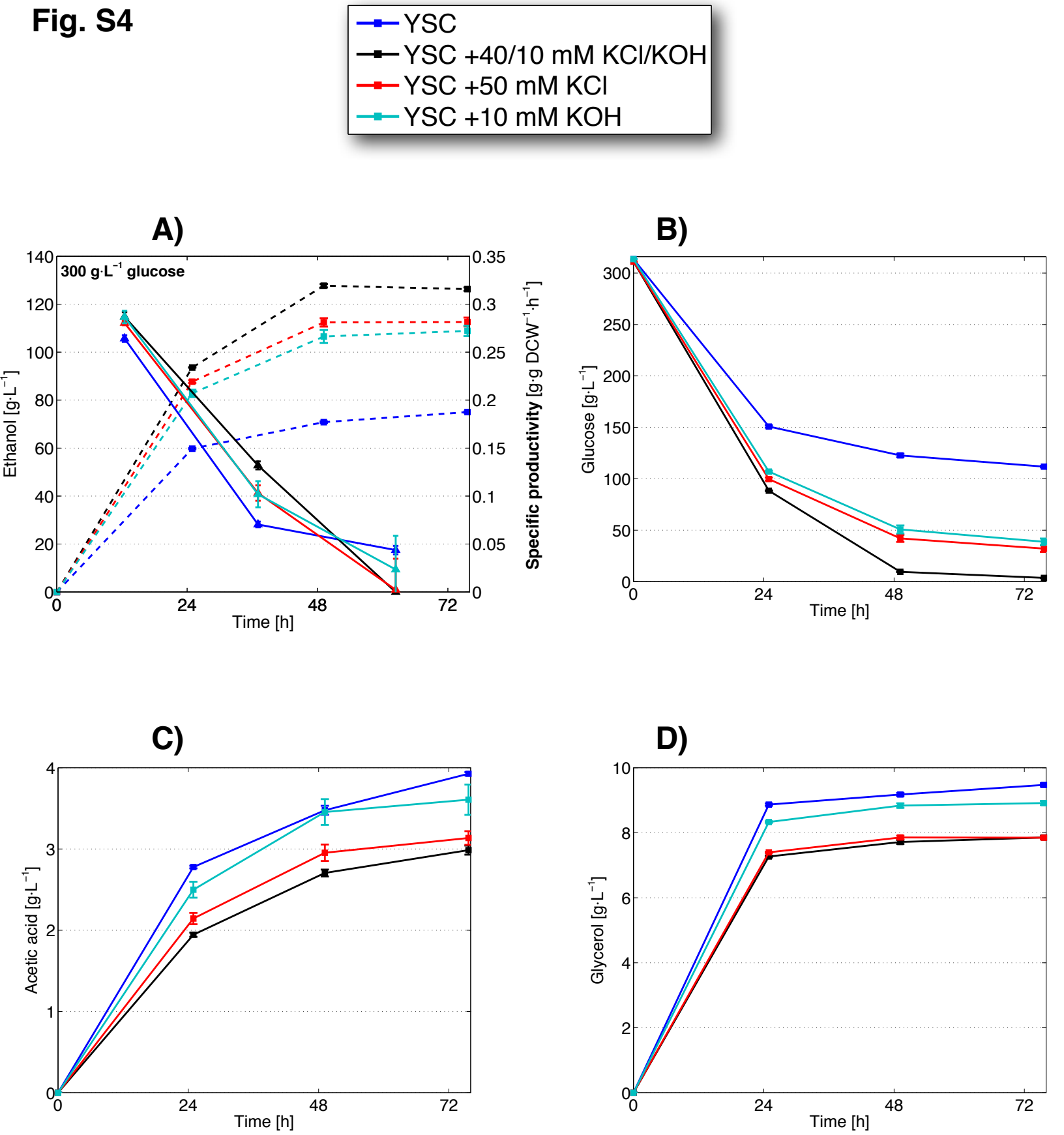

Fig. S4. Elevated potassium and pH (black) improve ethanol fermentation characteristics over equimolar potassium (red) or matched pH (cyan) alone. **(A)** Time course of ethanol production (dashed) and specific productivities (solid) calculated from the mean viable populations in fig. S5B. **(B, C, D)** Corresponding time courses of glucose consumption, acetate production, and glycerol production. Data are mean ± SD from 3 biological replicates.

Fig. S5 A)

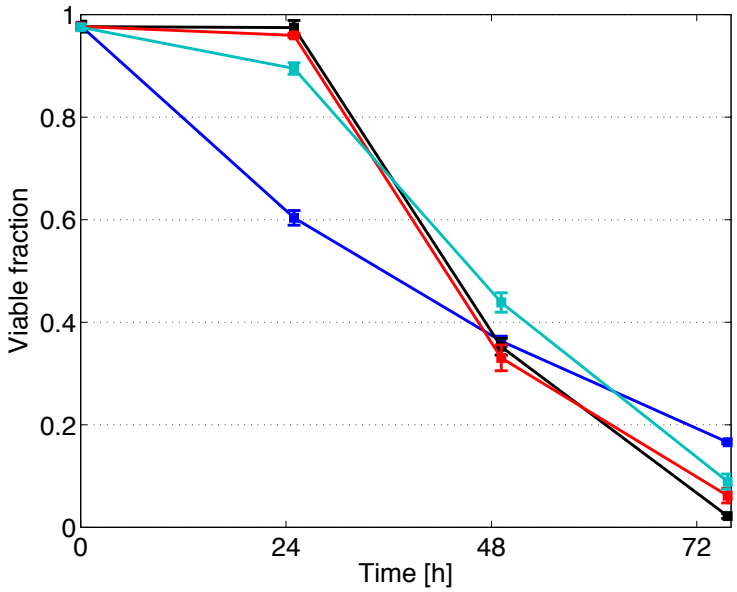

B)

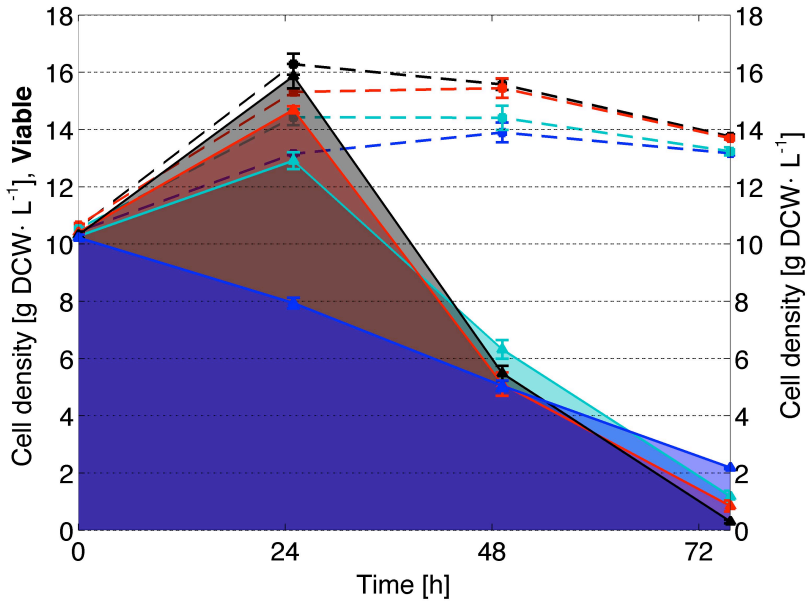

C)

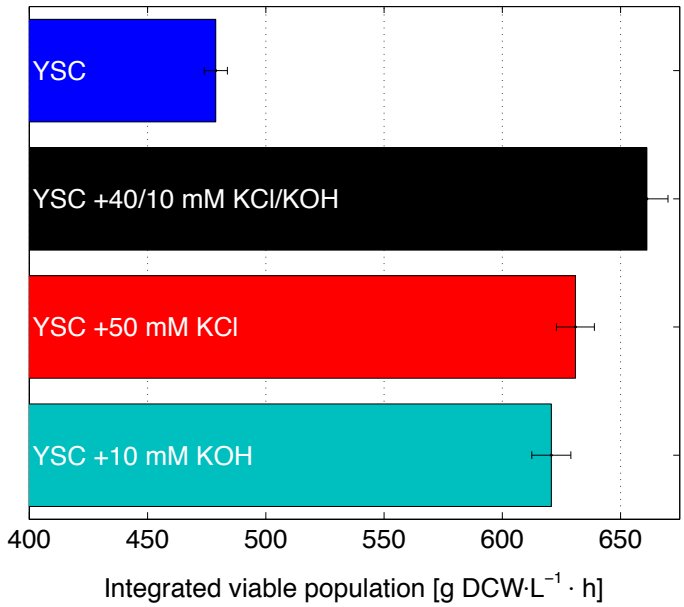

Fig. S5. Elevated potassium and pH (black) enhance ethanol tolerance over equimolar potassium (red) or matched pH (cyan) alone. **(A)** Viable cell fractions quantified from the fermentations in fig. S4. **(B)** Cell densities (dashed) and the corresponding underlying viable cell populations (solid) calculated from the fractions in **A**. Time integrals of the viable population (shaded) represent the net fermentation viability or total impact of supplementation on ethanol tolerance. **(C)** Quantification of the time integrals in **B**.

Fig. S6 A)

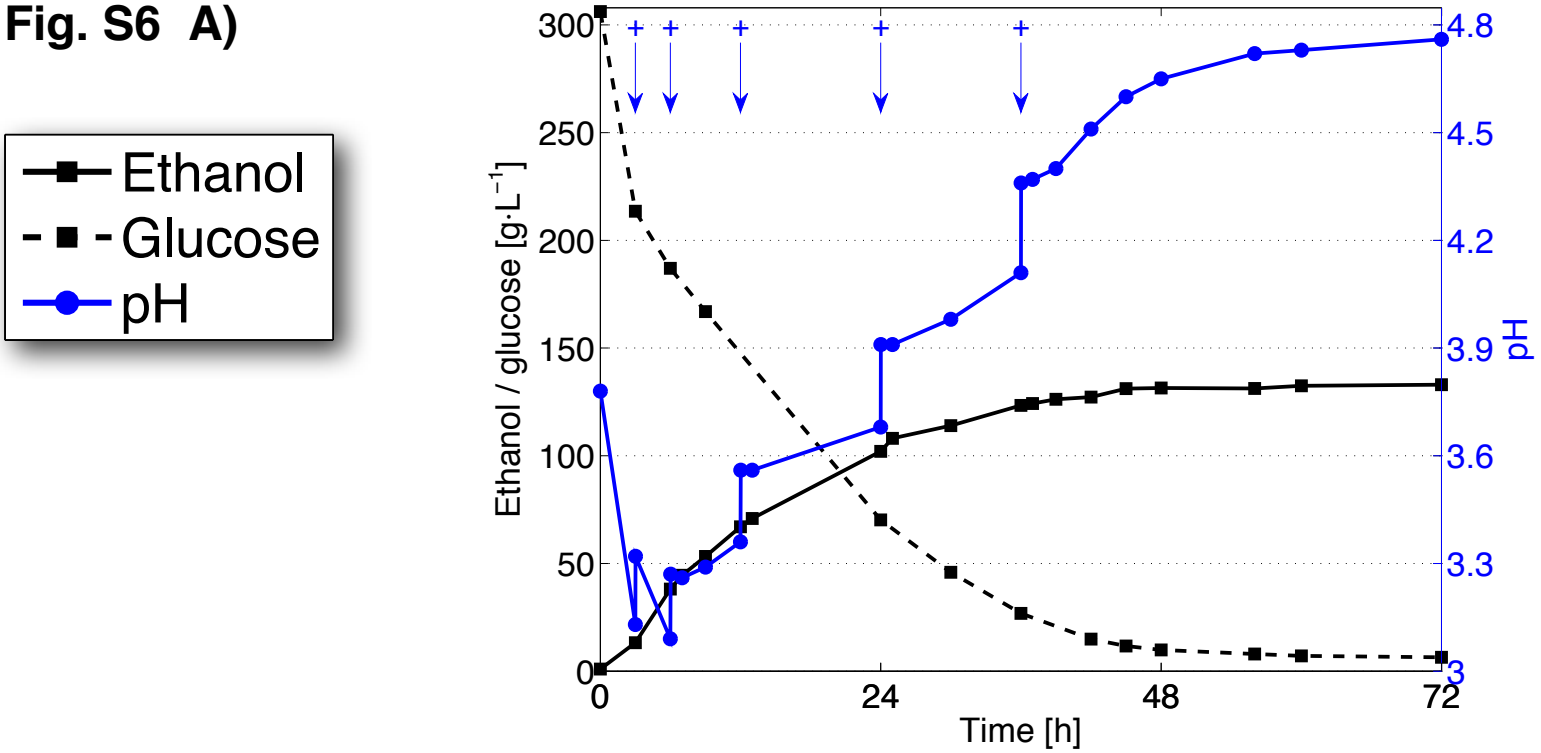

B)

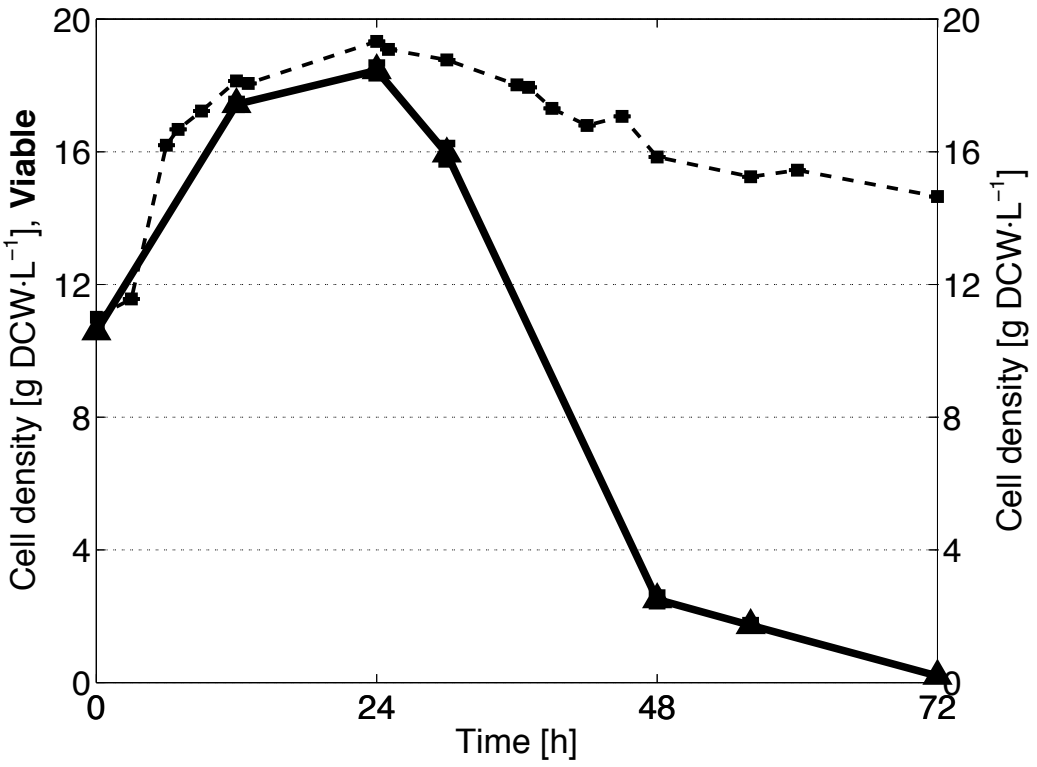

Fig. S6. Elevated potassium and pH enhance ethanol production in an anaerobic bioreactor environment. **(A)** Time course of ethanol production (black solid), glucose consumption (black dashed), and pH (blue). Manual additions of 2 mM KOH are indicated by blue arrows. **(B)** Corresponding time course of cell density (dashed) and the underlying viable cell population (solid).

Fig. S7 A)

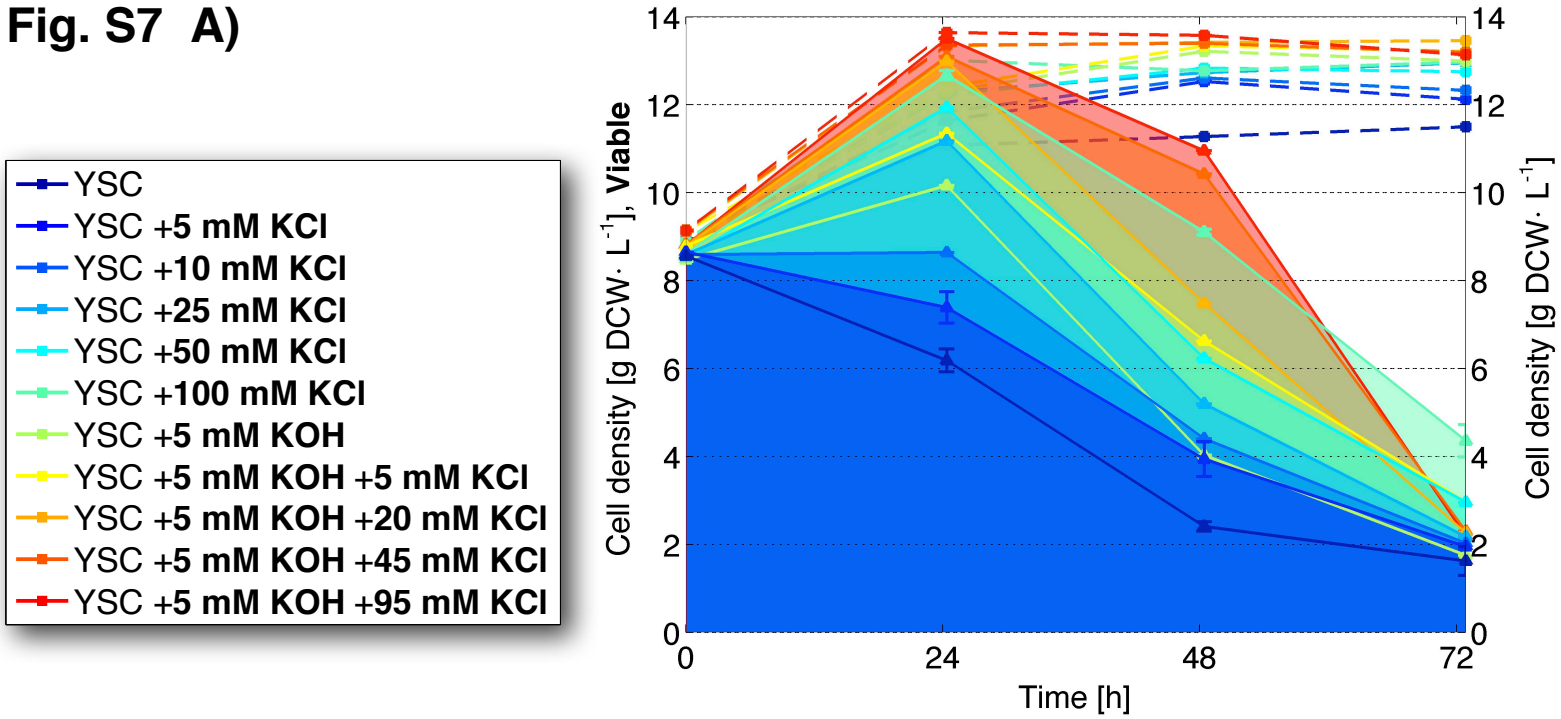

B)

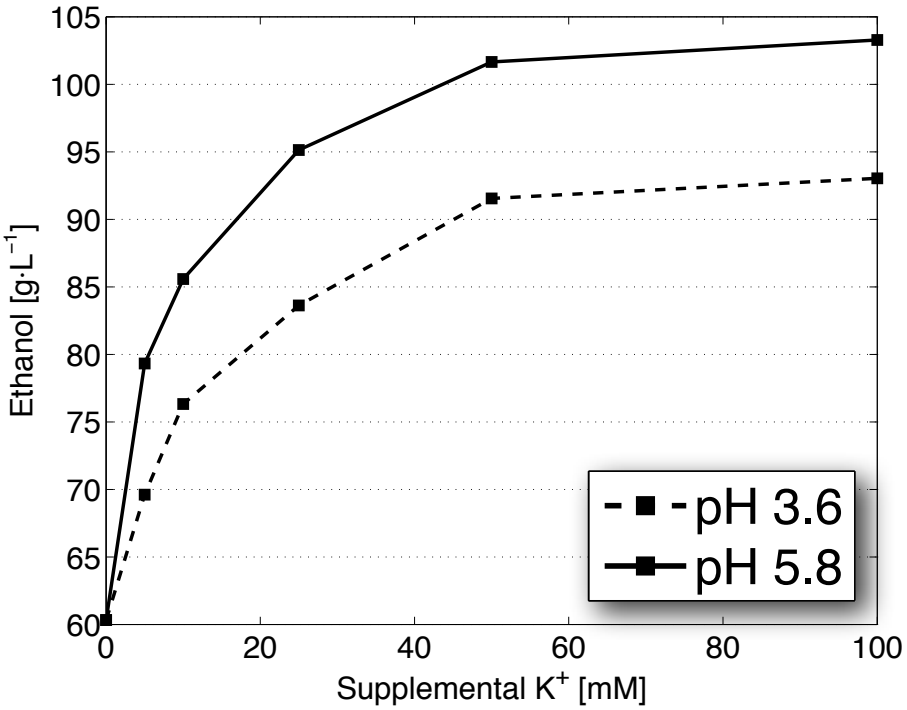

Fig. S7. Elevated potassium and pH exert saturable, dose-dependent improvements on ethanol tolerance and production. **(A)** Cell densities (dashed) and the corresponding time integrals of the viable cell population (shaded) from fermentations supplemented with 5–100 mM KCl (pH 3.6), or with 5 mM KOH and 5–95 mM KCl (i.e., equimolar potassium at pH 5.8). **(B)** Final ethanol titers of the fermentations in **A** shown as a function of supplemental potassium at the two pH values.

Fig. S8

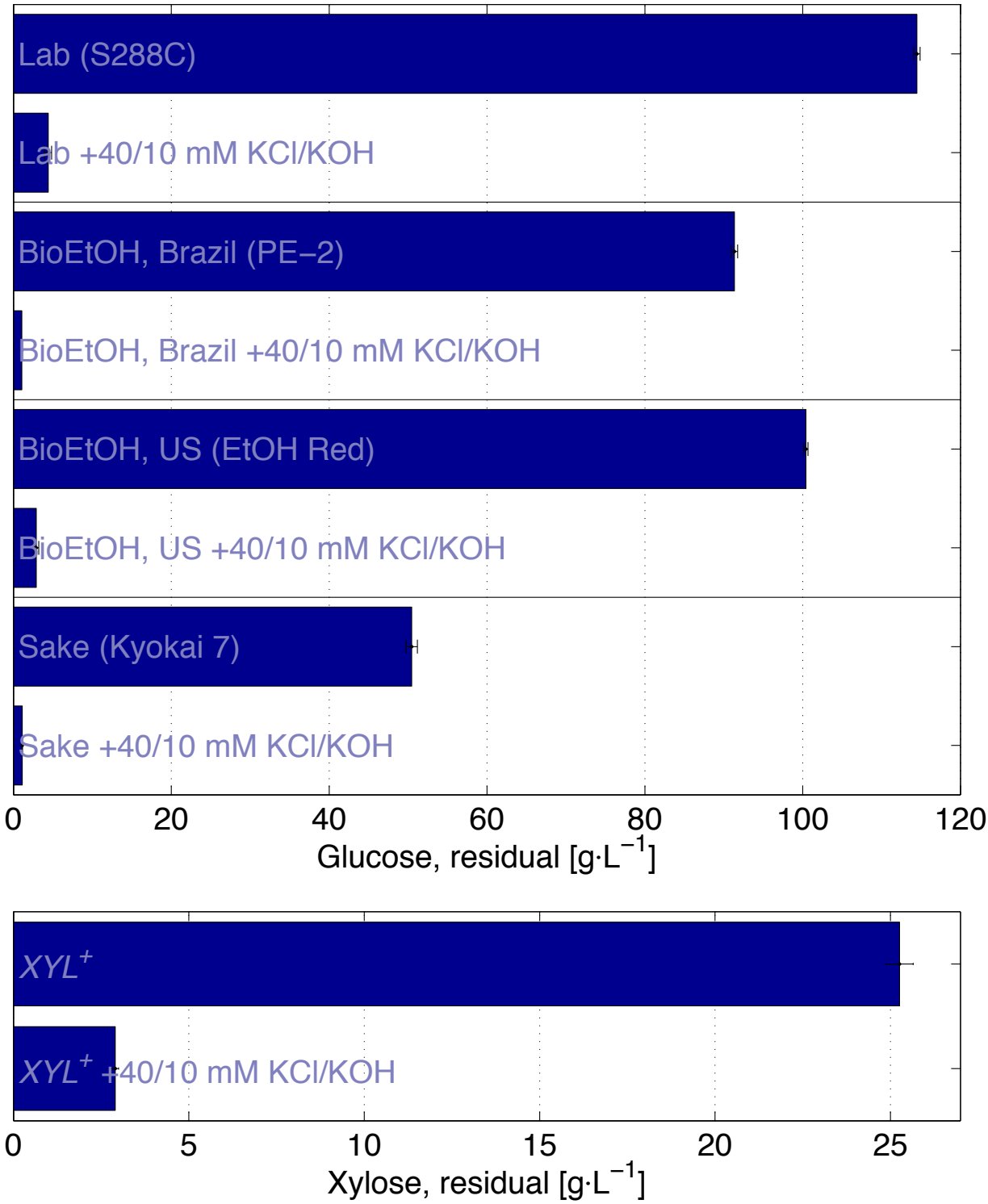

Fig. S8. Elevated potassium and pH are sufficient to induce complete consumption of fermentation sugar independently of strain genetics and sugar substrate. Residual sugar from glucose fermentation (top) of one laboratory (S288C) and three industrial (PE-2, Ethanol Red, Kyokai 7) yeast strains, or from xylose fermentation (bottom) of an engineered xylose strain, grown in unmodified YSC or YSC supplemented with 40 mM KCl and 10 mM KOH. Corresponding ethanol titers are shown in Fig. 2A. Data are mean ± SD from 3 biological replicates.

Fig. S9

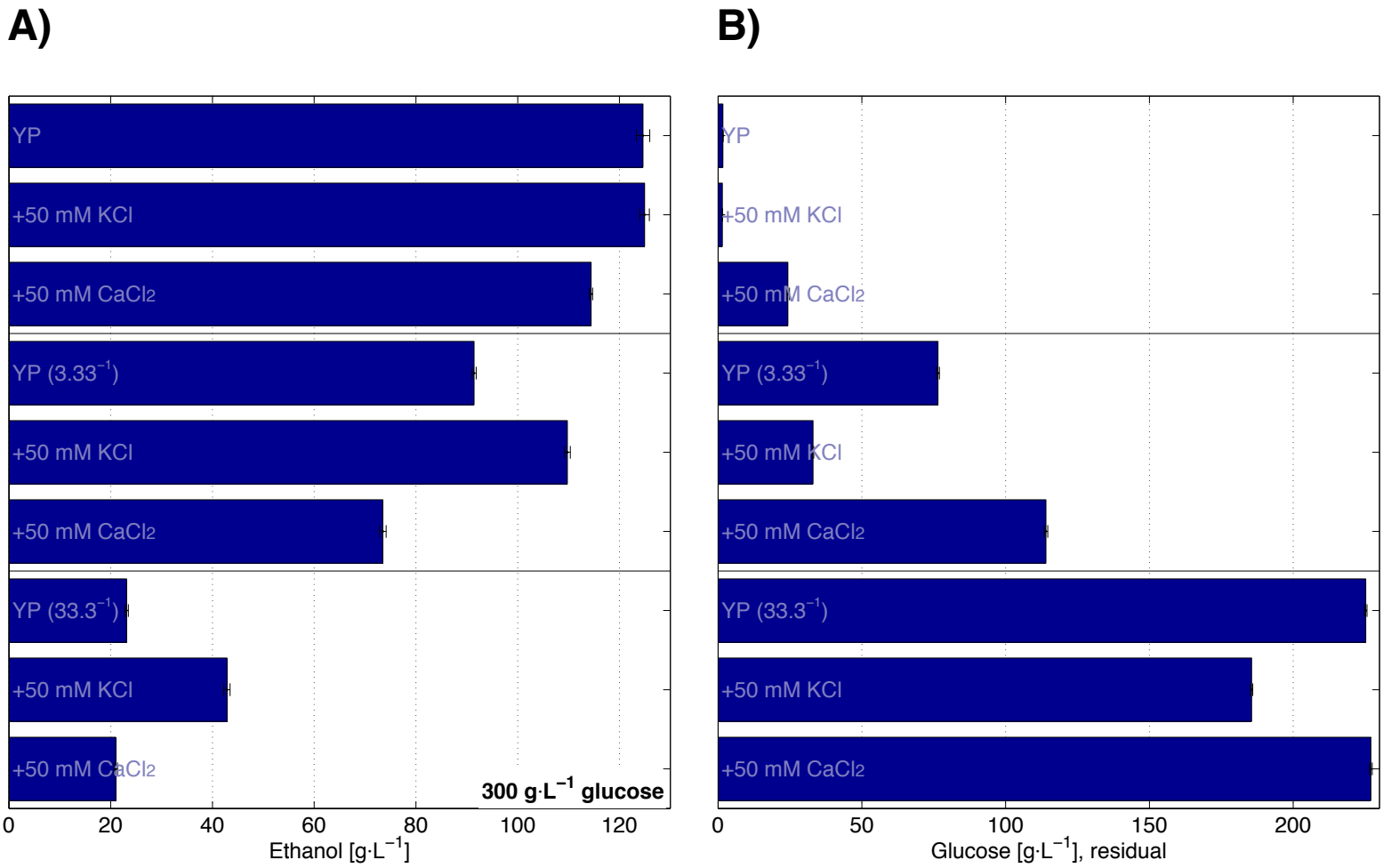

Fig. S9. Elevated potassium is sufficient to enhance fermentation in chemically undefined medium containing yeast extract and peptone (YP). **(A)** Ethanol titers from S288C cultured in undiluted YP, YP diluted to 30%, or YP diluted to 3%, all containing 300 g/L glucose and supplemented with either 50 mM potassium (as KCl) or calcium (as $CaCl_2$). **(B)** Residual glucose from the fermentations in **A**. Data are mean ± SD from 3 biological replicates.

Fig. S10A)

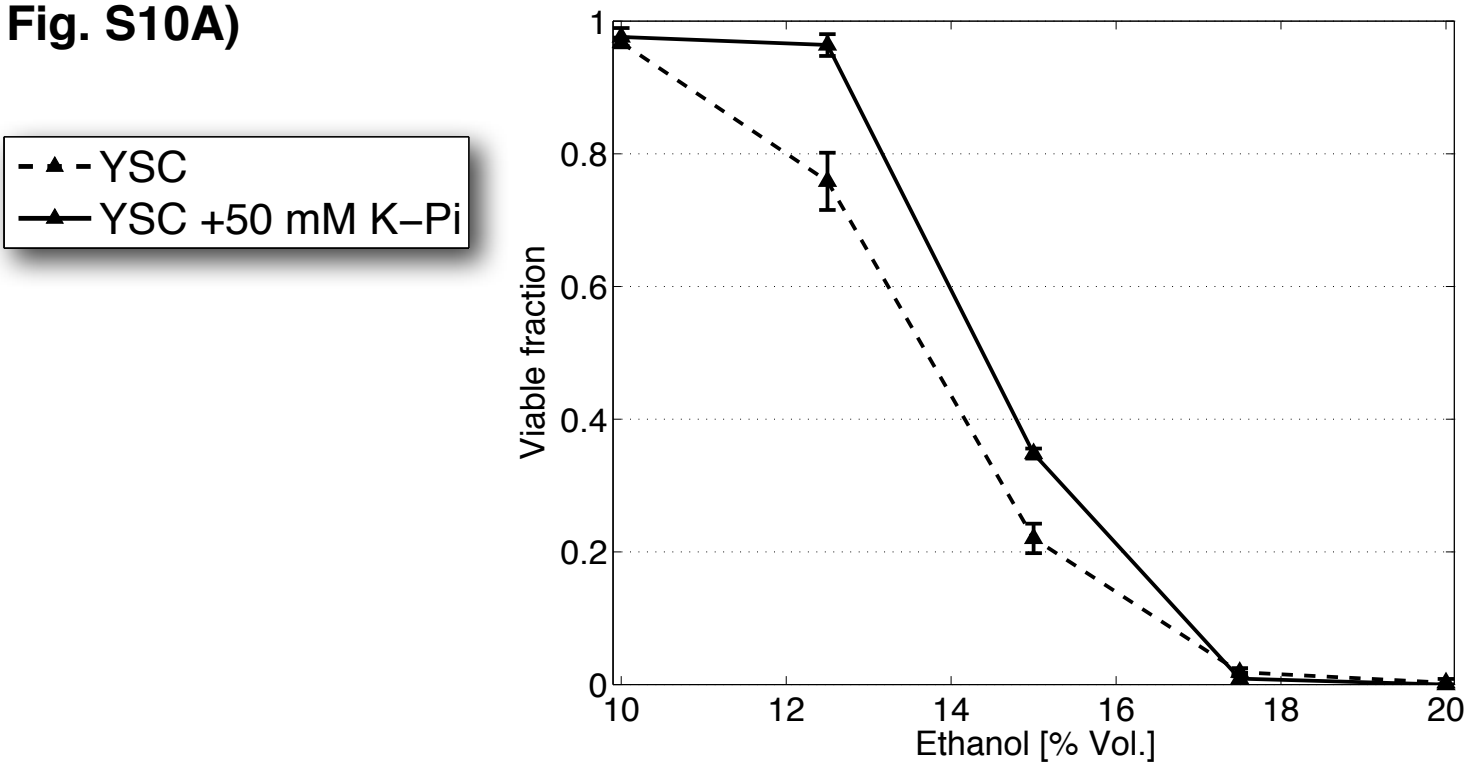

B)

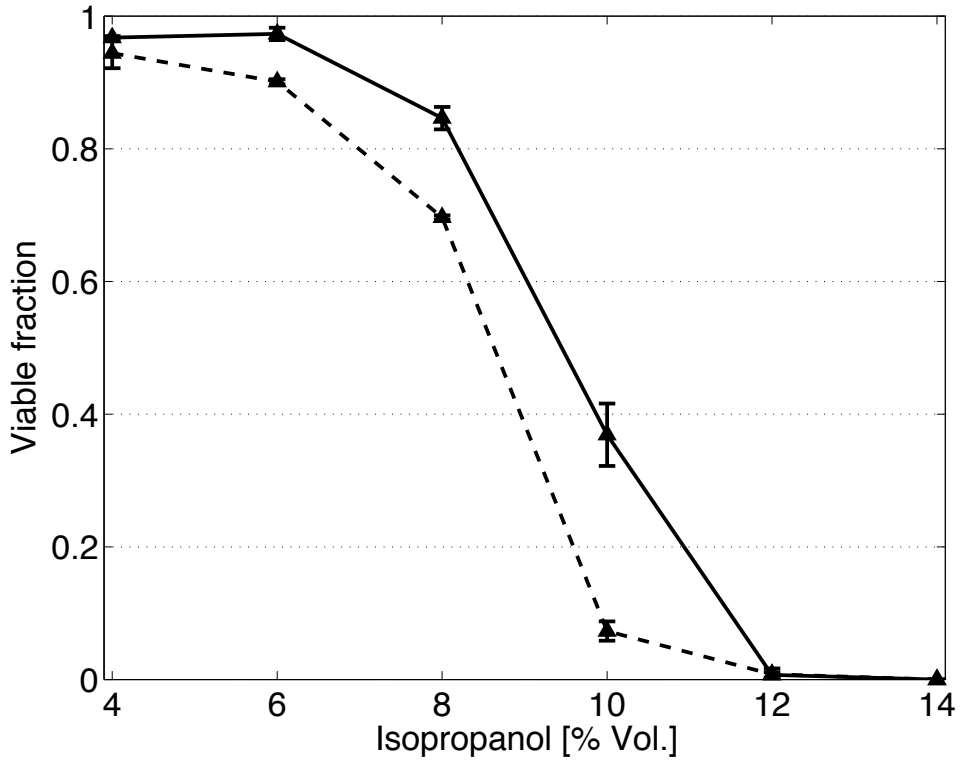

Fig. S10. Elevated potassium and pH are sufficient to enhance tolerance independently of alcohol species under high glucose conditions. **(A)** Population fractions surviving 135 min after transfer from overnight growth in unmodified YSC containing 300 g/L glucose (dashed), or that supplemented with 50 mM K-P_i (solid), into identical conditions containing the indicated concentrations of ethanol. **(B)** Same as **A**, but with steps of isopropanol and measurements after 4 h. Data are mean ± SD from 3 biological replicates.

Fig. S11

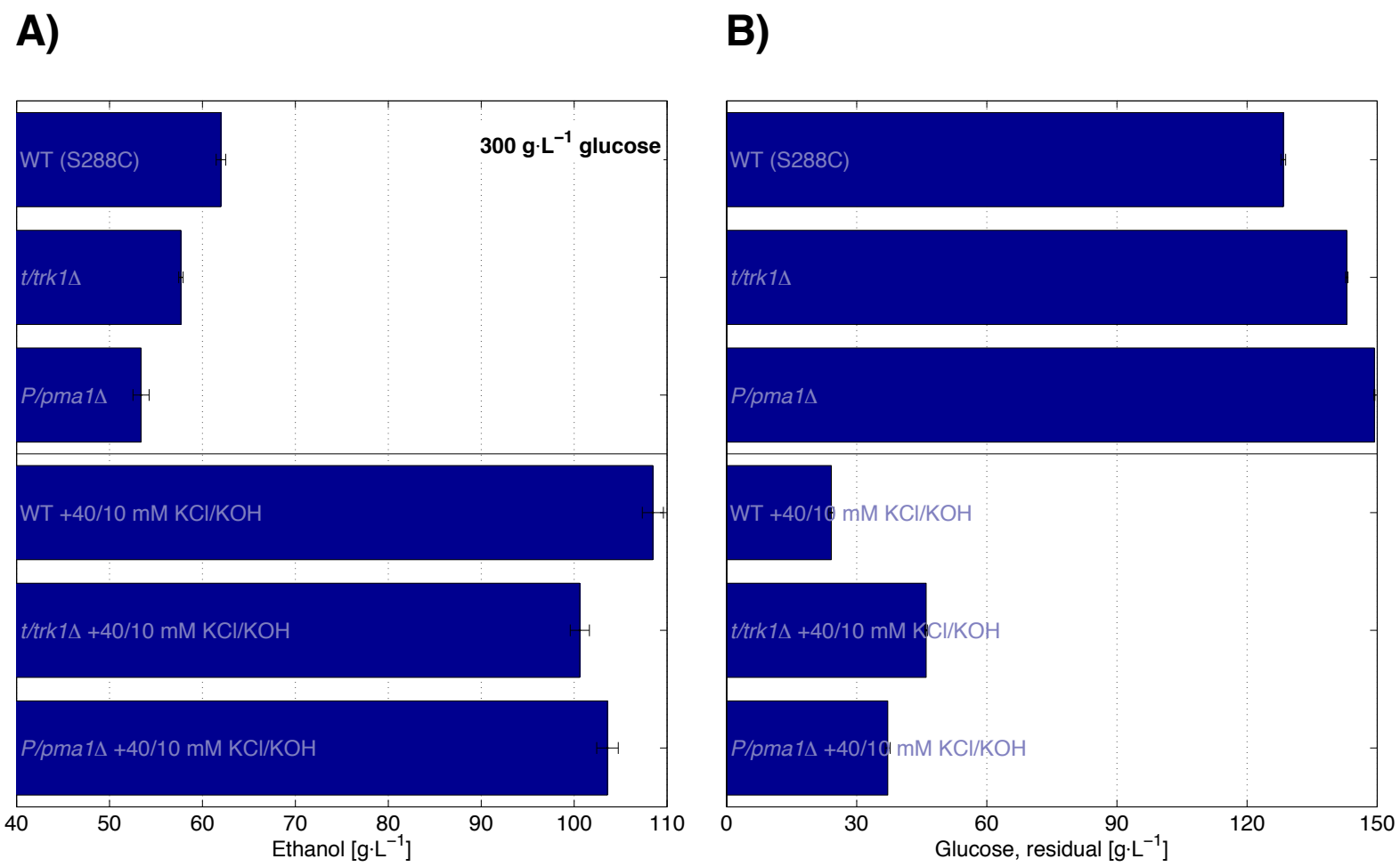

Fig. S11. Genetic impairment of potassium import or proton export decreases ethanol performance. **(A)** Ethanol titers from an auxotrophic wild type laboratory strain (S288C-based BY4743), an isogenic derivative harboring a homozygous deletion of the potassium pump (*trk1Δ/trk1Δ*), and an isogenic derivative with a heterozygous deletion of the proton pump (*PMA1/pma1Δ*), all cultured in unmodified YSC (top) or YSC supplemented with 40 mM KCl and 10 mM KOH (bottom). **(B)** Residual glucose from the fermentations in **A**. Data are mean ± SD from 3 biological replicates.

Fig. S12A)

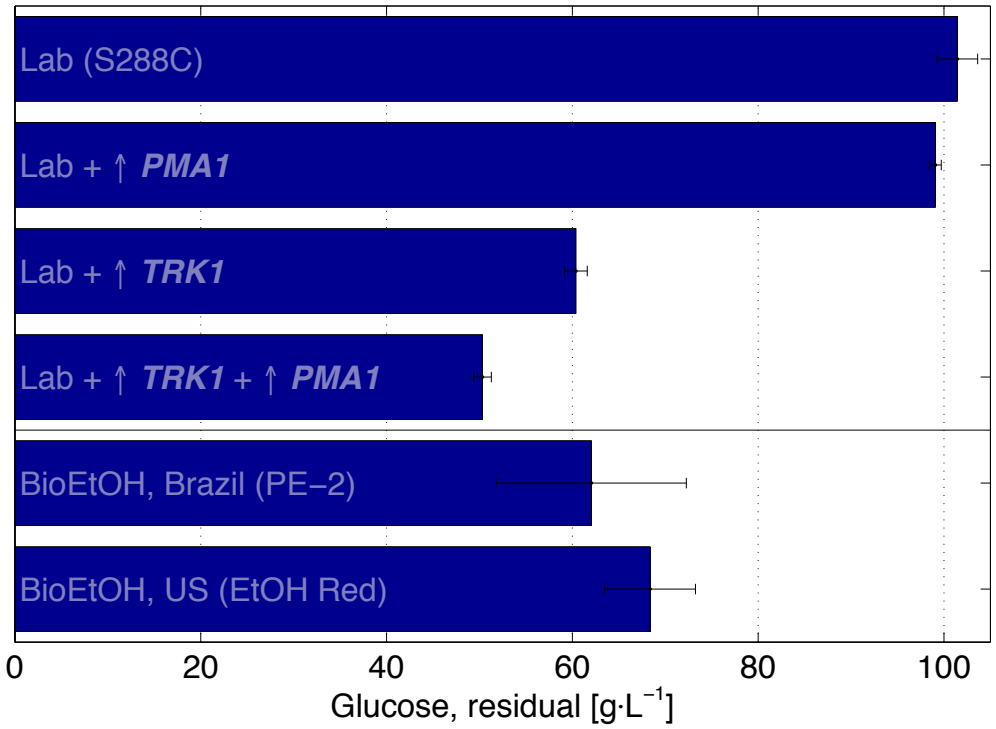

B)

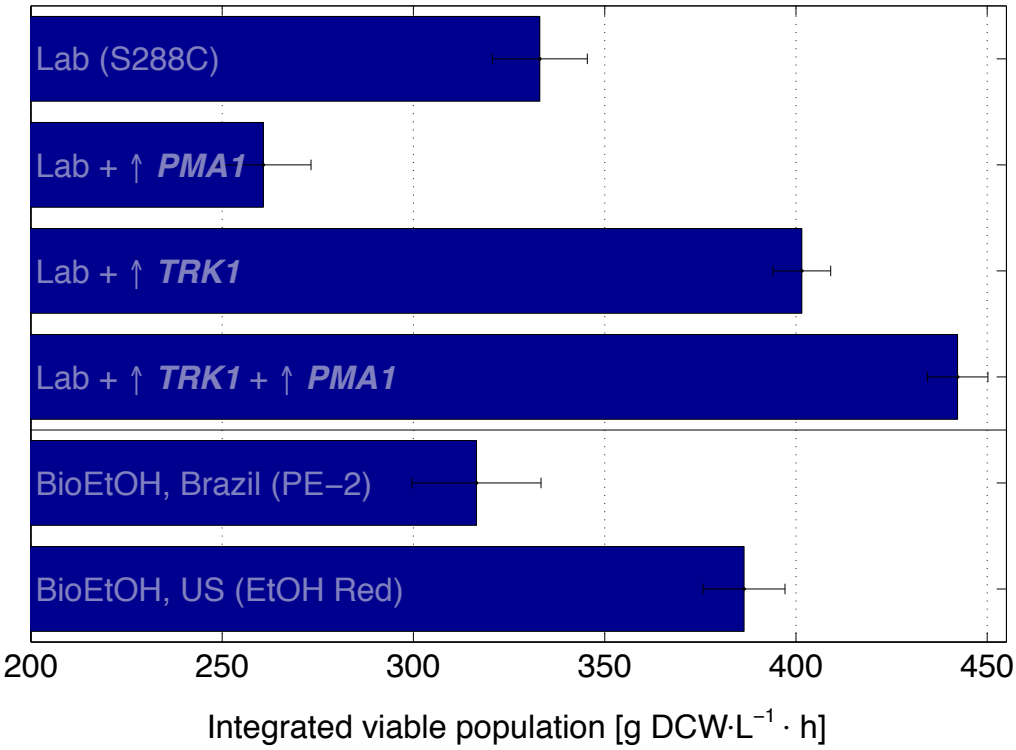

Fig. S12. Genetic augmentation of the plasma membrane potassium (*TRK1*) and proton (*PMA1*) pumps enhance ethanol tolerance and fermentation. **(A)** Residual glucose from a wild type laboratory strain (S288C) transformed with empty over-expression plasmid, S288C transformed with a plasmid over-expressing *PMA1*, S288C containing hyper-activated *TRK1* (via deletions of *PPZ1* and *PPZ2*) and transformed with empty over-expression plasmid, the *TRK1* hyper-activated strain transformed with a plasmid over-expressing *PMA1*, and bioethanol production strains from Brazil (PE-2) and the US (Ethanol Red), all cultured in unmodified YSC lacking uracil. Corresponding ethanol titers are shown in Fig. 3. **(B)** Net fermentation viability (time integrals of the viable population) from the fermentations in **A** and Fig. 3. Data are mean ± SD from 3 biological replicates.

Fig. S13A)

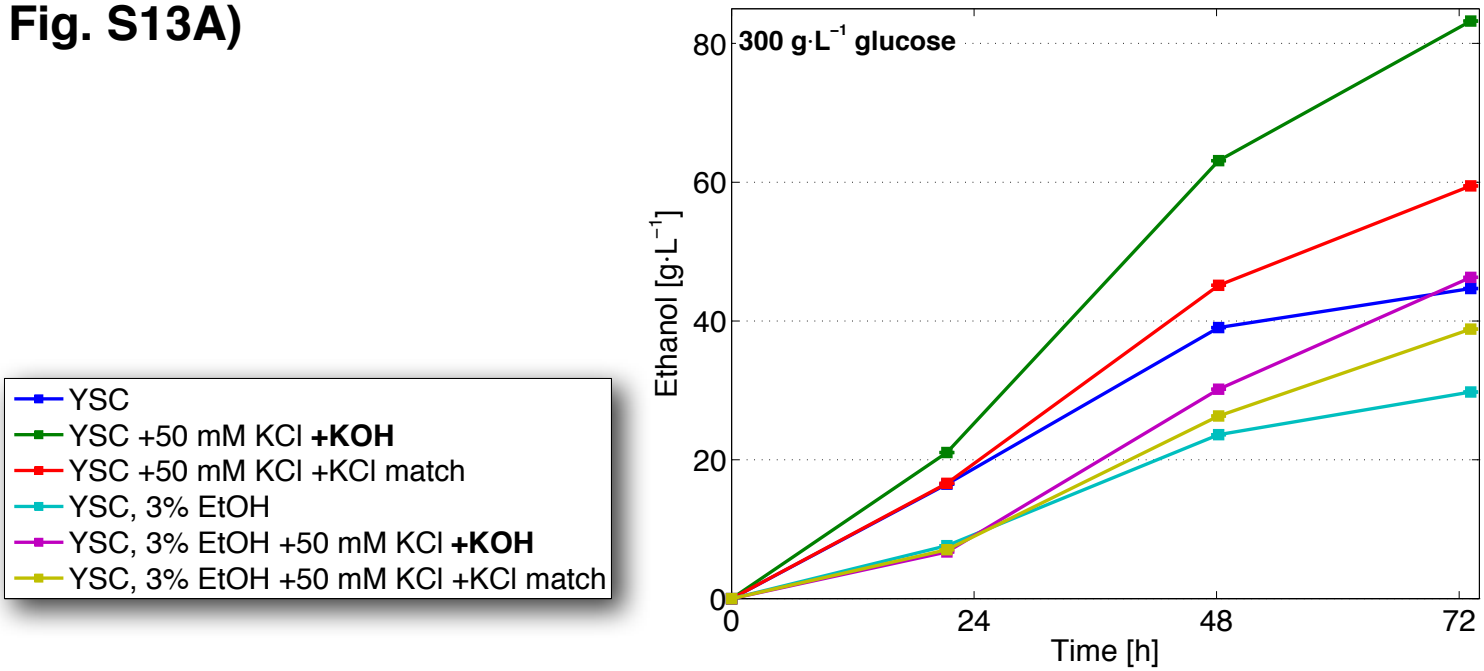

B)

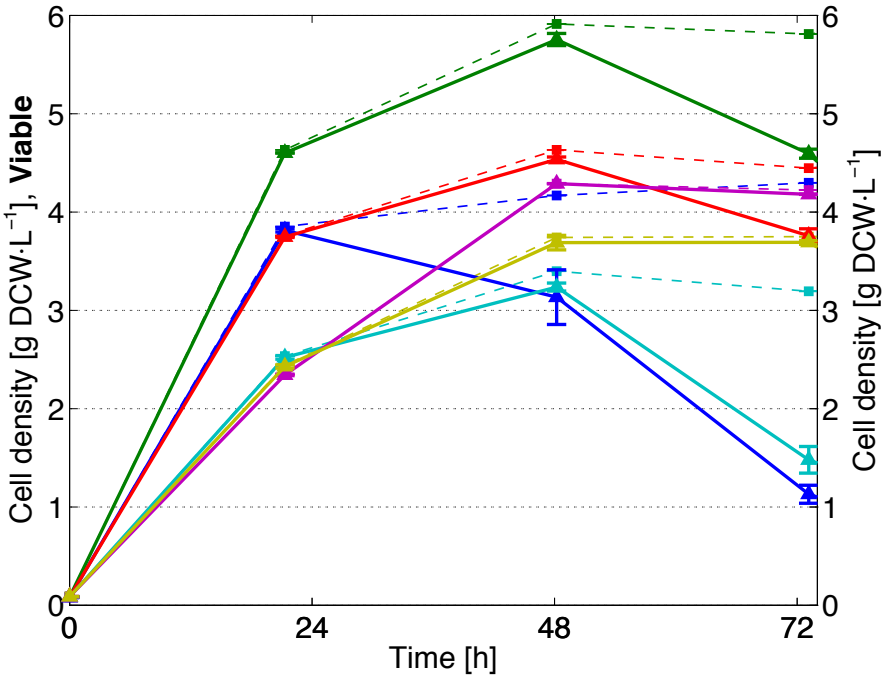

Fig. S13. Elevated potassium and pH enhance ethanol production and tolerance when nutrients remain in abundance, both in the absence and presence of a 3% ethanol stress. All cultures were equalized for initial pH (3.8) and cell density (OD_{600} = 0.1 or 0.04 g DCW/L). **(A)** Time course of ethanol production. **(B)** Time course of cell densities (dashed) and the underlying viable cell population (solid).

Table S1. Yeast strains.

Strain	Genotype	Reference
BY4743	S288C *MAT*a/α *his3Δ1/his3Δ1 leu2Δ0/leu2Δ0 LYS2/lys2Δ0 met15Δ0/MET15 ura3Δ0/ura3Δ0*	*(32)*
Ethanol Red	American bioethanol production strain (prototrophic)	Gift from Phibro Animal Health
FY4/5	S288C *MAT*a/α (prototrophic)	*(32)*
LAMy123	BY4743 p426TEF	This study
LAMy177	BY4743 *ppz1*Δ::kanMX4/*ppz1*Δ::kanMX4 *ppz2*Δ::kanMX4/*ppz2*Δ::kanMX4	This study
LAMy184	BY4743 p426TEF-*PMA1*	This study
LAMy189	LAMy177 p426TEF-*PMA1*	This study
LAMy191	LAMy177 p426TEF	This study
Kyokai No. 7 / NCYC 479	Sake brewing strain (prototrophic)	*(14)*
PE-2 / JAY270	Brazilian bioethanol production strain (prototrophic)	*(13)*
PMA1/*pma1*Δ	BY4743 *PMA1*/*pma1*Δ::kanMX4	*(33)*
*trk1*Δ/*trk1*Δ	BY4743 *trk1*Δ::kanMX4/*trk1*Δ::kanMX4	*(33)*
XYL^{+} / H131-A3-AL^{CS} / F283	BF264-15Dau, *TRP1::pTDH3-RKI1-tCYC1-pTDH3-RPE1-tCYC1, HIS2::pTDH3-TKL1-tCYC1, ADE1::pTDH3-PsTAL1-tCYC1* pUCAR1 pRS405	*(16)*

Table S2. Over-expression plasmids.

Plasmid	Insert	Reference
p426TEF	—	*(28)*
p426TEF-*PMA1*	*S. cerevisiae PMA1*	This study

Table S3. Fermentation conditions.

Fig.	Strain	Medium	Sugar (glucose / xylose) + Additive	$OD_{600,t0}$
1A-B	FY4/5	YSC	**glc:** 100 g/L → 150 g/L → 300 g/L ± 40 mM KCl + 10 mM KOH/KCl (during ferm.) ↳ 300 g/L + 10 mM KOH (during ferm.)	25
S4				
S5				
1C	FY4/5	YSC	**glc:** 100 g/L → 150 g/L → 300 g/L ± [5, 10, 25, 50, 100] mM KCl ↳ 300 g/L + 5 mM KOH ± [5, 20, 45, 95] mM KCl	22
S7				
2A	FY4/5	YSC	**glc:** 100 g/L → 150 g/L → 300 g/L ± 40 mM KCl + 10 KOH (during ferm.)	25
	PE-2	YSC	**glc:** 100 g/L → 150 g/L → 300 g/L ± 40 mM KCl + 10 KOH (during ferm.)	25
	Ethanol Red	YSC	**glc:** 100 g/L → 150 g/L → 300 g/L ± 40 mM KCl + 10 KOH (during ferm.)	25
S8	Kyokai No. 7	YSC	**glc:** 100 g/L → 150 g/L → 300 g/L ± 40 mM KCl + 10 KOH (during ferm.)	25
	H131-A3-AL^{CS}	YSC	**xyl**: 40 g/L → 60 g/L → 100 g/L ± 40 mM KCl + 10 KOH (during ferm.)	25
2B	FY4/5	YP (20%)	**glc:** 100 g/L → 150 g/L → 300 g/L ± 50 mM KCl (pH 6) ↳ 300 g/L ± 50 mM KCl (pH 3.7)	24
3	LAMy123	YSC –URA	**glc:** 100 g/L → 150 g/L → 300 g/L (Lab)	20
	LAMy184	YSC –URA	**glc:** 100 g/L → 150 g/L → 300 g/L (Lab + ↑ *PMA1*)	20
	LAMy191	YSC –URA	**glc:** 100 g/L → 150 g/L → 300 g/L (Lab + ↑ *TRK1*)	20
S12	LAMy189	YSC –URA	**glc:** 100 g/L → 150 g/L → 300 g/L (Lab + ↑ *TRK1* + ↑ *PMA1*)	20
	PE-2	YSC –URA	**glc:** 100 g/L → 150 g/L → 300 g/L (Bioethanol, Brazil)	20
	Ethanol Red	YSC –URA	**glc:** 100 g/L → 150 g/L → 300 g/L (Bioethanol, US)	20
S1	FY4/5	YSC	**glc:** 100 g/L → 150 g/L → 300 g/L ± 10 mM [L-histidine, L-leucine] ↳ 300 g/L + 50 mM [$CaCl_2$, LiCl, $MgCl_2$, KCl, KH_2PO_4, K_2HPO_4, K_2SO_4, NaCl, NaH_2PO_4, $NaCH_3COO$, Na_2SO_3]	25

Fig.	Strain	Medium	Sugar (glucose / xylose) + Additive	$OD_{600,t0}$
S2	FY4/5	YSC	**glc:** 100 g/L → 150 g/L → 300 g/L ± 50 mM KH_2PO_4 ↳ 300 g/L + 50 mM KCl +KOH (during ferm.) ↳ 300 g/L + 50 mM KCl +KCl (during ferm.)	23
S3	FY4/5	YSC	**glc:** 100 g/L → 150 g/L → 300 g/L ± 50 mM [KCl, KH_2PO_4, K_2SO_4, NaCl, NaH_2PO_4] ↳ 300 g/L + 40 mM KCl + 10 mM KOH (during ferm.) ↳ 300 g/L + 40 mM NaCl + 10 mM NaOH (during ferm.)	25
S6	FY4/5	YSC	**glc:** 100 g/L → 150 g/L → 300 g/L + 40 mM KCl + 10 KOH (during ferm.)	27
S9	FY4/5	YP	**glc:** 100 g/L → 150 g/L → 300 g/L ± 50 mM [$CaCl_2$, KCl]	26
		YP (30%)	**glc:** 100 g/L → 150 g/L → 300 g/L ± 50 mM [$CaCl_2$, KCl]	26
		YP (3%)	**glc:** 100 g/L → 150 g/L → 300 g/L ± 50 mM [$CaCl_2$, KCl]	26
S11	BY4743	YSC	**glc:** 100 g/L → 150 g/L → 300 g/L ± 40 mM KCl + 10 KOH (during ferm.)	23
	*trk1*Δ/*trk1*Δ	YSC	**glc:** 100 g/L → 150 g/L → 300 g/L ± 40 mM KCl + 10 KOH (during ferm.)	23
	PMA1/*pma1*Δ	YSC	**glc:** 100 g/L → 150 g/L → 300 g/L ± 40 mM KCl + 10 KOH (during ferm.)	23
S13	FY4/5	YSC	**glc:** 100 g/L → 150 g/L → 300 g/L ± 3% ethanol ↳ 300 g/L ± 3% ethanol + 50 mM KCl +KOH (during ferm.) ↳ 300 g/L ± 3% ethanol + 50 mM KCl +KCl (during ferm.)	0.1